NASA CR- 144739

[redacted]

(NASA-CR-144739) A SIMULATION FOR GRAVITY FINE STRUCTURE RECOVERY FROM LOW-LOW GRAVSAT SST DATA Final Report (Business and Technological Systems, Inc.) 87 p HC $5.00 CSCL 22C G3/17

N76-21251

Unclas 21571

BUSINESS AND TECHNOLOGICAL SYSTEMS, INC.

BTS

BTS-TR-76-29

January 1976

A SIMULATION FOR GRAVITY FINE STRUCTURE RECOVERY FROM LOW-LOW GRAVSAT SST DATA

R. H. Estes (BTS)

and

E. R. Lancaster (GSFC)

FINAL REPORT

Contract NAS 5-20901

Prepared for

NATIONAL AERONAUTICS AND SPACE ADMINISTRATION
Goddard Space Flight Center
Greenbelt, Maryland 20771

by

BUSINESS AND TECHNOLOGICAL SYSTEMS, INC.
Aerospace Building, Suite 605
10210 Greenbelt Road
Seabrook, Maryland 20801

1. Report No.	2. Government Accession No.	3. Recipient's Catalog No.
4. Title and Subtitle A SIMULATION FOR GRAVITY FINE STRUCTURE RECOVERY FROM LOW-LOW GRAVSAT SST DATA		5. Report Date January 1976 6. Performing Organization Code
7. Author(s) R. H. Estes (BTS) and E. R. Lancaster (GSFC)		8. Performing Organization Report No. BTS-TR-76-29
9. Performing Organization Name and Address Business and Technological Systems, Inc. 10210 Greenbelt Road, Suite 605 Seabrook, Maryland 20801		10. Work Unit No. 11. Contract or Grant No. NAS 5-20901
12. Sponsoring Agency Name and Address National Aeronautics and Space Administration Goddard Space Flight Center Greenbelt, Maryland 20771		13. Type of Report and Period Covered Final Report 14. Sponsoring Agency Code
15. Supplementary Notes		

16. Abstract

Covariance error analysis techniques were applied to investigate estimation strategies for the low-low SST mission for accurate local recovery of gravitational fine structure, considering the aliasing effects of unsolved for parameters. A 5° x 5° surface density block representation of the high order geopotential was utilized with the drag-free "low-low" GRAVSAT configuration in a circular polar orbit at 250 km altitude. Recovery of local sets of density blocks from long data arcs was found not to be feasible due to strong aliasing effects. The error analysis for the recovery of local sets of density blocks using independent short data arcs demonstrated that the estimation strategy of simultaneously estimating a local set of blocks covered by data and two "buffer layers" of blocks not covered by data greatly reduced aliasing errors. However, for the low-low configuration the SST data type exhibits strong satellite state recovery ability only for the along track component of velocity, the normal matrix being poorly conditioned for the recovery of radial and cross track components. This requires satellite orbital accuracies from other tracking means to a minimum of 10 meters in position and .01 meters/sec in radial and cross track velocity components.

17. Key Words (Selected by Author(s))	18. Distribution Statement
Covariance Error Analysis Geopotential Fine Structure Satellite-to-Satellite Tracking	

19. Security Classif. (of this report)	20. Security Classif. (of this page)	21. No. of Pages	22. Price*
Unclassified	Unclassified	83	

*For sale by the Clearinghouse for Federal Scientific and Technical Information, Springfield, Virginia 22151.

TABLE OF CONTENTS

1.0 INTRODUCTION

The concept of the "low-low" GRAVSAT satellite to satellite tracking mission has been proposed as a technique for helping to determine the fine structure of the earth's gravity field. The system consists of two drag-free satellites separated by a few hundred kilometers in the same low altitude polar orbit constrained to follow a purely gravitational path. Such a satellite configuration is highly sensitive to geopotential variations, and the polar circular orbit would provide continuous tracking over the entire earth, with either one or both satellites having tracking capability and ability to transmit telemetry to the earth. The tracked satellite would have an ordinary spacecraft transponder.

The physical reason for sensitivity to local gravity perturbations in the "low-low" configuration is clear. As the two satellites approach a gravitational perturbation, the nearer satellite "feels" its presence sooner and experiences an acceleration relative to its sister satellite. When the first satellite passes the perturbation, its acceleration changes sign relative to its sister, and as it recedes from the perturbation, the acceleration it "feels" diminishes. The sister satellite experiences a similar acceleration, but out of phase with the first satellite. The projection of the difference between their velocities along the separation vector, the satellite-to-satellite range rate, then has a definite signature for the satellite configuration and the gravity perturbation. Gravity perturbations far from the two satellites tend to act on each satellite in the same manner and hence produce little relative velocity (Figure 1).

Highly accurate gravity models are needed for two purposes: to accurately predict satellite motion and to determine the detailed shape of the geoid. NASA's Earth and Ocean Physics Program (EOPAP) will require a determination of the geoid to 10 cm, together with an orbital prediction accuracy in satellite altitude to 10 cm. The requirement placed on the accuracy of the gravitational fine structure necessitates an extremely large number of parameters in the gravity field model. A simultaneous data reduction for all model parameters would be a tremendously difficult computer task, even with the most sophisticated new computer systems. The range rate data between the two satellites in the "low-low" configuration, however, is highly sensitive to local gravity perturbations and much less sensitive to gravity perturbations distant from the satellite pair. This supports the attractive idea of representing the gravitational fine structure in a local

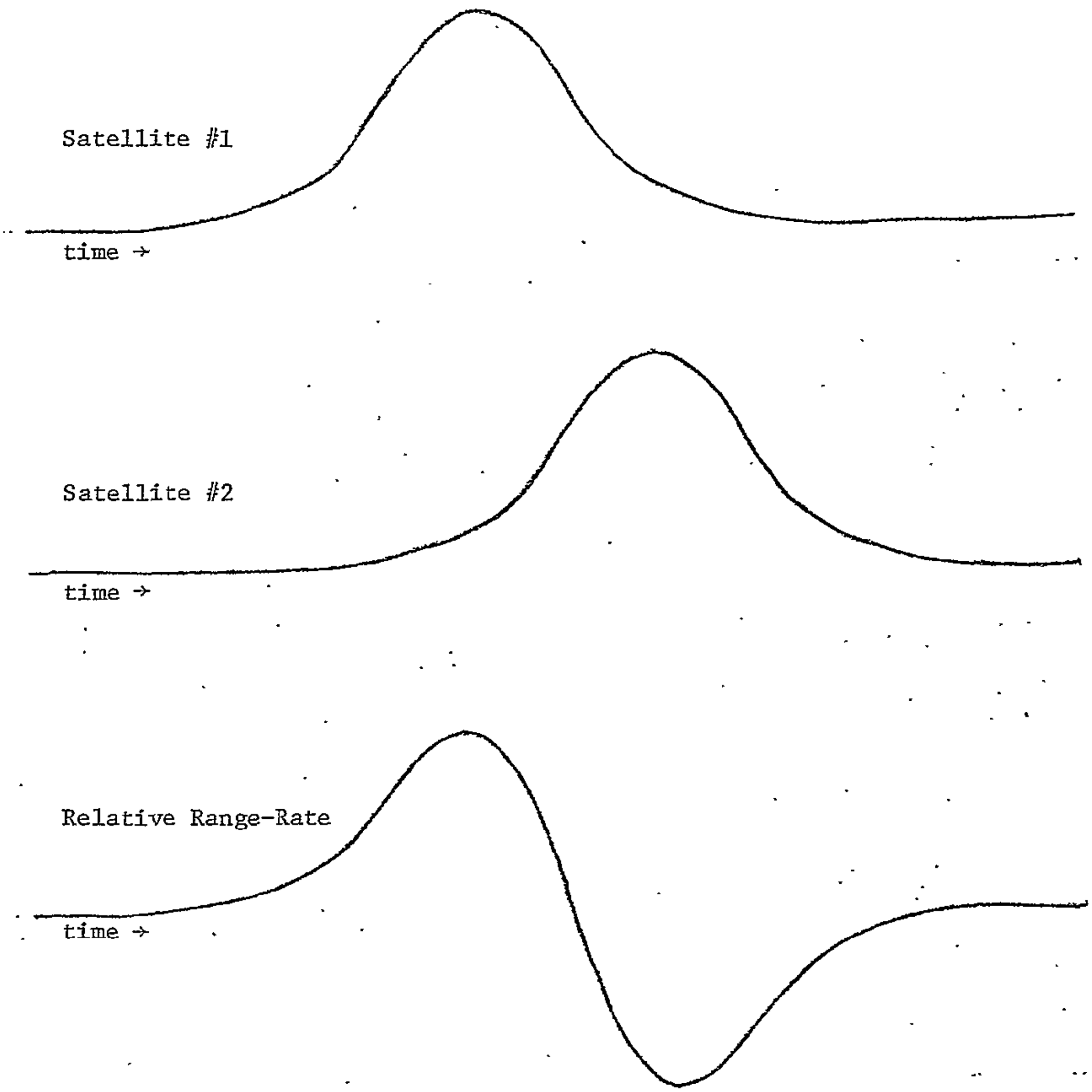

FIGURE 1 The top two curves diagram the change in velocity magnitude as a function of time as the low-low satellites pass over a perturbing anomaly. The bottom curve is the difference of the top curves, showing the approximate shape of the relative range-rate signal between the spacecraft caused by the perturbation.

mathematical model and estimating a local area of gravitational perturbations using local data. This would, of course, require a fewer number of model parameters and make the problem more manageable. The global solution could then be built up from a set of these local solutions. This idea has been tested by simulation for SST data by Schwarz [9] and Hajela [4].

Schwarz utilized specially developed software for least squares parameter estimation to study the feasibility of the "low-low" and "high-low" mission with *summed* SST range and range-rate data, i.e. the measurement proceeded from a ground station to the tracking satellite to the tracked satellite and back again. He selected surface density blocks to represent the high order gravity field above a truncated spherical harmonic reference field and limited his study to a geographically isolated set of these blocks. Data was simulated over the blocks and a least squares estimating process attempted to recover the surface density parameters. His study processed only short data arcs and solved for only the surface density block parameters. The orbit states were considered to be nuisance parameters and were not estimated. A serious shortcoming of his study was neglecting the contaminating effects of errors in non-estimated neighboring surface density blocks on the accuracy of the estimated blocks. We refer to this as aliasing.

Hajela, using the GEODYN program [2] performed a similar feasibility study for the "high-low" mission using equal area gravity anomaly blocks to represent the high order gravity field. Again using simulated *summed* SST range and range-rate data he attempted a least squares recovery of local sets of gravity anamoly blocks using multiple short arcs of data. Unlike Schwarz, he included the aliasing effects of errors in neighboring blocks on the estimated blocks by including in his estimated solution a band of blocks around the perimeter of the blocks of interest and outside of the data coverage. In his study, Hajela essentially assumed that he knew the satellite states perfectly by assigning them very small a priori sigmas in the estimation algorithm. Whereas Schwarz performed all of his least squares adjustments using infinite a priori sigmas for the surface density blocks, Hajela included in his investigation cases where a priori information for the gravity anomaly blocks was assumed.

The purpose of this investigation is to apply covariance error analysis techniques to determine under what estimation strategies the "low-low" mission is feasible for local recovery of gravitational fine structure when the effects of aliasing are considered. This investigation treats 5^{o} x 5^{o} surface blocks with the satellite altitudes at 250 km. Other studies (Schwarz [9], Lowrey [8]) have investigated the sensitivity to and resolvability of surface features of given size as a function of the "low-low" orbital altitude. The drag compensation system of the GRAVSAT satellite has been assumed to be error free in this study, so that the results obtained will be somewhat optimistic. In a more detailed and realistic study the aliasing effect in the parameter estimation due to imperfect knowledge of surface force compensation must be included.

2.0 SURFACE DENSITY GEOPOTENTIAL REPRESENTATION

The purpose for the present study of the low-low SST experiment is to determine the feasibility of recovering the fine structure of the earth's gravity field as a composite of recoveries over local regions. The total geopotential is represented as

$$W = U + T$$

where the function U is assumed to be a fixed low order reference field and T represents the high order potential.

The potential T could be expressed by any one of several mathematical models, i.e. spherical harmonics, gravity anomalies, sampling functions, spherical grid, etc. Whatever model is chosen, the description of the gravity fine structure will require a very large set of parameters. For example, 2° geoid resolution would require in excess of 8400 spherical harmonic coefficients. While the "low-low" SST experiment will provide global data coverage and the simultaneous estimation of the full parameter set is theoretically possible, it represents a very large and difficult numerical task for even the largest computers. While a complete study of such a global fine structure estimation is worthwhile, it will not be pursued in this investigation. Instead we attempt to estimate subsets of parameters while keeping the remainder at a priori values. The complete solution is then built up from these subset solutions. However, unless the parameterization exhibits local independence or "orthogonality" with respect to the data type, the uncertainties in the neglected parameters will badly alias the adjusted parameters and such a recovery procedure will not be possible. Orthogonality has been defined by Argentiero [1] as follows: For a given estimation procedure, the jth adjusted parameter is orthogonal to the kth unadjusted parameter if the aliasing contribution of k to j is zero.

We have selected to parameterize the high order geopotential by local surface density blocks representing a fictitious surface density layer,

$$T = \iint_{\sigma} \frac{G\rho \, d\sigma}{d}$$

where G is the gravitational constant, $d\sigma$ is the element of surface area, ρ is the density of the mass layer and d is the distance from the point where T is evaluated to the integration element $d\sigma$. The parameter used to describe the high order field is $\Phi \equiv G\rho$ with units of acceleration. The value of the parameter Φ will be expressed in milligals (mgal), where

$$1 \text{ mgal} = 10^{-3} \text{ gals} = 10^{-3} \text{cm/sec}^2 \quad .$$

The relationship of the parameter Φ to gravity anomalies Δg is given approximately by (Heiskanen and Moritz, page 303)

$$\Phi = \frac{1}{2\pi} (\Delta g + \frac{3}{2} g \frac{N}{R})$$

where g is the mean normal gravity, N is the geoid undulation and R is the mean earth radius. For order of magnitude comparisons between the surface density parameter Φ and corresponding gravity anomalies, the expression

$$\Phi = \frac{\Delta g}{2\pi}$$

is adequate. A detailed treatment of the surface layer potential is given by Schwarz, including transformations between the density layer representation and spherical harmonic and gravity anomaly representations. For simplicity, the mass layer is considered spread on the surface of a sphere with radius equal to the mean radius of the earth.

The density layer is modeled by individual area blocks in which the density is a constant value representing the average density of the surface layer within the block. The disturbing potential is then

$$T = \sum_j \Phi_j \iint_{\sigma_j} \frac{1}{d_j} d\sigma_j$$

where the integration is over the area of the jth block and the sum is over all surface blocks. The integral over each block is evaluated by dividing the block into a number of sub-blocks of area σ_{jk}, where the distance d_{jk} is the distance from the center of the sub-block to the point of evaluation,

ORIGINAL PAGE IS
OF POOR QUALITY

$$T = \sum_j \Phi_j \sum_k \frac{\sigma_{jk}}{d_{jk}} .$$

Note that this is equivalent to representing the potential of each block by the sum of the potentials of a point mass located at the center of each sub-block, with mass $\Phi_j \sigma_{jk}/G$. The accuracy with which this summation of sub-blocks represents the integral over the block depends, of course, on the number of sub-blocks used. For satellite distances which are large compared to the block size, a single mass point approximation is suitable, whereas for satellite disturbances which are of the same order as the block size, many mass points are needed (Figure 2).

The principal portion of this investigation is concerned with recovering local subsets of blocks utilizing surface blocks with boundaries defined by constant values of latitude and longitude increments (equalangular blocks). Such blocks have areas which are strongly dependent on latitude, e.g. a 5° x 5° block on the equator possesses a larger area, and hence produces a larger perturbation for a given surface density, than a 5° x 5° block at a different latitude.

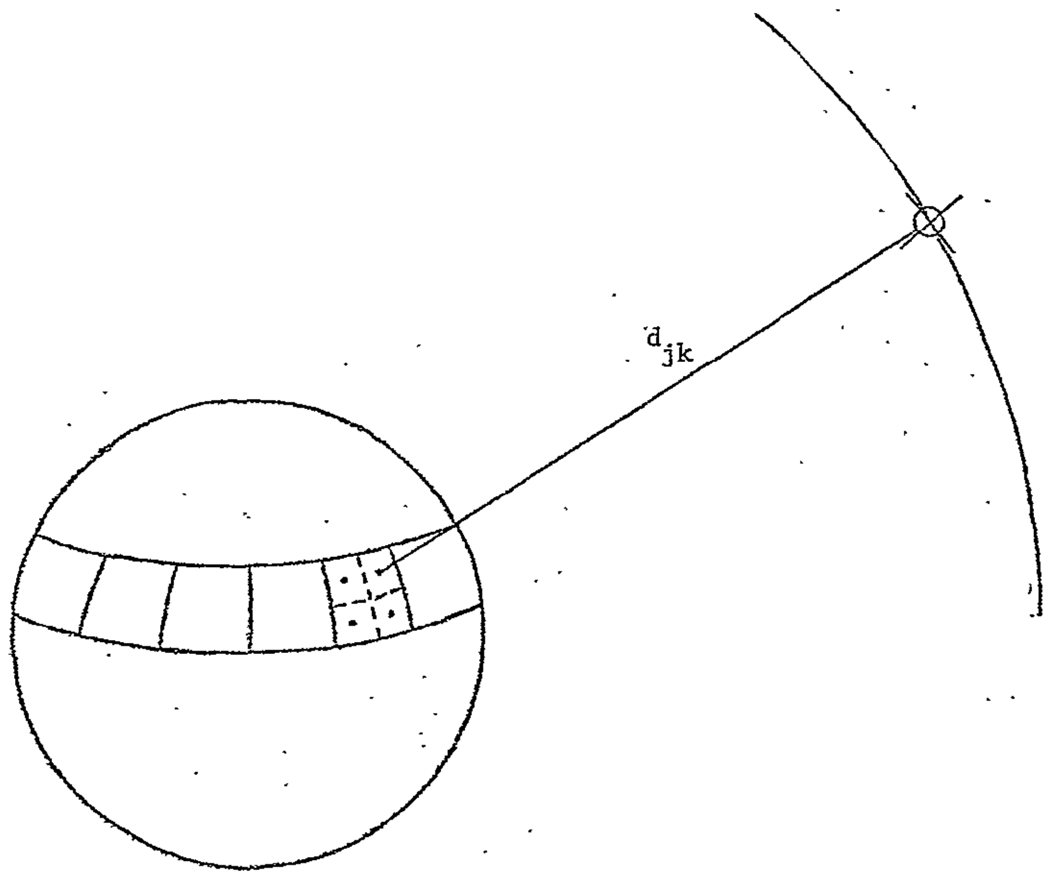

FIGURE 2   Subdivision of surface density blocks into sub-block point mass approximations for numerical evaluation.

3.0 COMPUTER SOFTWARE DESIGN

In an effort to utilize existing software in the investigation, where possible, several existing orbital estimation/error analysis computer programs were considered: GEODYN/ERODYN, NAP/NAPCOV, ORAN and GTDS. Constraints placed on the ultimate choice of software were:

1) Adequate documentation.
2) Capability for a large set of adjusted parameters.
3) Multi-arc/multi-satellite processing.
4) SST data type.
5) Surface density force model.
6) Data generation capability.
7) Parameter estimation capability.
8) Error analysis capability.
9) Availability of program for modification.

Although none of the systems available filled all needs, the program most appropriate was determined to be GEODYN/ERODYN.

GEODYN is a large scale orbital parameter estimation program oriented toward geodynamical applications, while ERODYN is an orbital and geodetic error analysis program designed to be operated directly from GEODYN output. To perform an error analysis of the GEODYN estimation algorithm, ERODYN requires the estimation normal matrix output from GEODYN. Moreover, to investigate by error analysis the partitioning of a parameter set into adjust and unadjust (alias) parameters, the total parameter set must be adjusted in a GEODYN run so that all parameters are included in the normal matrix. This normal matrix, obtained from a single GEODYN run, is then partitioned into appropriate adjust and unadjust sets within ERODYN. The setting of a priori parameter sigmas and the partitioning of the total parameter set into adjust and unadjust parameters within ERODYN permits a great many error analysis runs to be made from a single GEODYN normal matrix.

As the surface density gravity model and the SST data type capability were a little used portion of the GEODYN program, extensive checking of these features was performed and program errors corrected. The variational equations were checked by numerical secant partials, i.e. by incrementing the initial state and surface density parameters and integrating the state vector so that partial derivatives could be formed relative to the nominal state vector.

The relative range and range-rate measurements between the two satellites and the measurement partials are calculated by the program in terms of the difference between the state vectors of the satellites and the geometric and variational partials

$$\rho = \sqrt{(\bar{X}_2-\bar{X}_1)\cdot(\bar{X}_2-\bar{X}_1)}$$

$$\dot{\rho} = \frac{(\bar{X}_2-\bar{X}_1)\cdot(\dot{\bar{X}}_2-\dot{\bar{X}}_1)}{\rho}$$

$$\begin{aligned}\frac{\partial\rho}{\partial\Phi_i} &= \frac{\partial\rho}{\partial\bar{X}_1}\frac{\partial\bar{X}_1}{\partial\Phi_i} + \frac{\partial\rho}{\partial\bar{X}_2}\frac{\partial\bar{X}_2}{\partial\Phi_i} \\ &= \frac{\partial\rho}{\partial\bar{X}_2}\left(\frac{\partial\bar{X}_2}{\partial\Phi_i} - \frac{\partial\bar{X}_1}{\partial\Phi_i}\right)\end{aligned}$$

$$\begin{aligned}\frac{\partial\dot{\rho}}{\partial\Phi_i} &= \frac{\partial\dot{\rho}}{\partial\bar{X}_1}\frac{\partial\bar{X}_1}{\partial\Phi_i} + \frac{\partial\dot{\rho}}{\partial\bar{X}_2}\frac{\partial\bar{X}_2}{\partial\Phi_i} + \frac{\partial\dot{\rho}}{\partial\dot{\bar{X}}_1}\frac{\partial\dot{\bar{X}}_1}{\partial\Phi_i} + \frac{\partial\dot{\rho}}{\partial\dot{\bar{X}}_2}\frac{\partial\dot{\bar{X}}_2}{\partial\Phi_i} \\ &= \frac{\partial\dot{\rho}}{\partial\bar{X}_2}\left(\frac{\partial\bar{X}_2}{\partial\Phi_i} - \frac{\partial\bar{X}_1}{\partial\Phi_i}\right) + \frac{\partial\dot{\rho}}{\partial\dot{\bar{X}}_2}\left(\frac{\partial\dot{\bar{X}}_2}{\partial\Phi_i} - \frac{\partial\dot{\bar{X}}_1}{\partial\Phi_i}\right)\end{aligned}$$

where the state vectors and variational partials are integrated separately for each satellite. Calculating relative motion quantities in such a manner can lead to important significant digits being lost in the subtraction. As a check on the numerical accuracy maintained, a closure test was performed on both the satellite state vector and variational partials. By closure we mean the integrating of the system of differential equations forward in time from an initial solution X_o at time t_o to a solution X_f at time t_f, and then reversing the time direction and integrating backward from the solution X_f at time t_f to a solution X_o' at time t_o. A comparison of X_o and X_o' reveals the accuracy of the integration process. Our simulation for satellite orbits of interest for the "low-low" mission using an 11th order Cowell integrator disclosed that 12 significant digits in the satellite state and 9 digits in the variational equations were retained when $t_f - t_o$ was set at 8 hours and an integration step size of 20 seconds was used. This accuracy assures 4 to 5 significant digits in calculated relative motion quantities, which is adequate for error analysis purposes. However, for future *estimation/recovery* purposes using relative range or range-rate SST data, it will probably be necessary to integrate the system of orbital equations for the relative state vector, where appropriate rearrangement has been performed to eliminate the subtraction of nearly equal quantities [3], [7].

GEODYN, as indicated, is primarily a scientific tool for geodetic and geodynamical study and is not easily implemented for mission analysis needs. In particular, there is no efficient data simulation capability in the system. To fulfill the needs of this study significant modifications to the GEODYN system version 7410.0 were performed, rendering it a more applicable mission study software system. This version of GEODYN with the mission analysis capability updates has been denoted GEOMAP, Geodynamics and Mission Analysis Program. Some of the modifications to the GEODYN/ERODYN system for the performance of this study include:

- SST range, range-rate, summed range and summed range-rate data generation.
- Selection of simulated data by data type, time intervals, and geographic latitude and longitude limits for the ground track.
- Equal-area surface density blocks.
- Additive random noise for simulated data.
- Simplified user input for surface density blocks.
- Simplified force model evaluation for surface density blocks.
- Multi-arc capability for ERODYN.
- Triple precision matrix inversion routine for ERODYN.

- HCL (radial, cross track, along track) state vector a priori sigma input for ERODYN.

Modification to the force model evaluation for surface density blocks was made in an effort to reduce computer time. The effect of a surface density block is modeled in the program by a user specified number of mass points symmetrically placed within the block. However, only blocks near the satellites need such accurate mathematical representation and blocks far from the ground track may be modeled much more simply. GEOMAP has been implemented to offer three options:

1. All surface blocks represented by the same number of user specified mass points.

2. All surface blocks within a cone defined by a user specified geocentric angle from the subsatellite point represented by the user prescribed number of mass points, and blocks outside of this angle represented by a single mass point.

3. All surface blocks outside a given angular cone of the subsatellite block completely neglected. This option may be used in conjunction with options 1. or 2.

Option 2 is similar to the technique implemented in later versions of GEODYN where the number of mass points representing the blocks inside of the cone is set to 9 and is not a user input.

As implemented at the time of this study, ERODYN operated as a single arc error analysis package. Multi-arc capability was added by modifying a program made available by Dr. P. Argentiero (private communication) designed to concatenate single arc normal matrices into a single larger dimensional normal matrix suitable for analysis by the linear algebra capability of ERODYN. This leads to some degree of inefficiency in that blocks of zeros are introduced into the concatenated normal matrix which are subject to mathematical computations. However, as a means to quickly add multi-arc error analysis capability to ERODYN for the purposes of this study it is entirely adequate.

In light of the modifications made to GEODYN Version 7410.0 and to avoid possible confusion, the software system used for this study will be designated GEOMAP/ERODYN in the remainder of this report.

4.0 COVARIANCE ERROR ANALYSIS DESCRIPTION

The error analysis for the Bayesian least squares estimator in GEODYN is described in the ERODYN Program Mathematical Description [5]. However, for completeness we reproduce the main points of the mathematical treatment.

Let y be an n dimensional vector of observations modeled by the nonlinear equation

$$y = F(X,S) + \varepsilon$$

where X and S are parameters of the dynamical system. Here X denotes the parameter set to be adjusted (estimated) and S denotes the parameter set which is unadjusted, or constrained to constant values in the estimation process but whose uncertainties are to be considered in computing the covariance matrix of the estimate. The vector ε represents the observation noise, which is mean zero and statistically independent. Linearizing about a nominal solution of the parameters X_N and S_N yields

$$\delta y = C \begin{bmatrix} \delta X \\ \\ \delta S \end{bmatrix} + \varepsilon$$

$$= A\delta X + B\delta S + \varepsilon$$

where

$$\delta y = y - F(X_N, S_N)$$

$$\delta X = X - X_N$$

$$\delta S = S - S_N$$

$$A = \left. \frac{\partial F(X,S)}{\partial X} \right|_{X_N, S_N}$$

$$B = \left.\frac{\partial F(X,S)}{\partial S}\right|_{X_N, S_N}$$

and

$$C = \begin{bmatrix} A & 0 \\ 0 & B \end{bmatrix}$$

Here X and S denotes the actual values of the adjusted and unadjusted parameters. and $\delta X_a = X - X_a$ represents the difference between the actual and a priori values of the adjusted parameters.

The normal matrix for all parameters is given by

$$n = C^T W C$$

$$= \begin{bmatrix} A^T WA & A^T WB \\ B^T WA & B^T WB \end{bmatrix}$$

where the weight matrix W is the inverse of the observation noise covariance matrix and is assumed to be diagonal, i.e.

$$W^{-1} = E(\varepsilon\varepsilon^T) = \begin{bmatrix} \sigma_1^2 & & 0 \\ & \ddots & \\ 0 & & \sigma_n^2 \end{bmatrix}$$

where E denotes expected values and σ_i is the ith observation noise sigma.

The Bayesian least squares estimate of X is given by

$$\hat{\delta X} = (A^T WA + P_a^{-1})^{-1} A^T W \delta y + (A^T WA + P_a^{-1})^{-1} P_a^{-1} \hat{\delta X}_a$$

where

$$\hat{\delta X}_a = X_a - X_N$$

and

$$P_a = E[(X_a - X)(X_a - X)^T]$$

is the covariance matrix of the a priori estimate X_a. Substitutions yield the error

$$\Delta X = \hat{\delta X} - \delta X = (A^T W A + P_a^{-1})^{-1} (A^T W B \delta S + A^T W \varepsilon - P_a^{-1} \delta X_a)$$

showing the three distinct components due to aliasing, measurement noise, and a priori uncertainties.

Under the assumption that δS, ε, and δX_a are uncorrelated errors, the covariance matrix of the adjusted parameters is given by

$$P \equiv E[(\hat{X}-X)(\hat{X}-X)^T] = (A^T W A + P_a^{-1})^{-1}$$

$$+ (A^T W A + P_a^{-1})^{-1} (A^T W B) V_S (B^T W A) (A^T W A + P_a^{-1})^{-1}$$

where V_S is the diagonal covariance matrix of the unadjusted parameters,

$$V_S = E(\delta S \delta S^T) \quad .$$

The sensitivity matrix of adjusted to unadjusted parameters is

$$\mathcal{S} = \frac{\partial \Delta X}{\partial \delta S} = (A^T W A + P_a^{-1})^{-1} A^T W B$$

so that the aliasing error to the ith adjusted parameter due to the jth unadjusted parameter is

$$\sigma_{ij} = \mathcal{S}_{ij} \, \sigma_{S_j} \, .$$

The ith diagonal element of P, or the variance of the ith adjusted parameter is then given by

$$\sigma_i^2 = \left[(A^T W A + P_a^{-1})^{-1}_{ii}\right] + \sum_j (S_{ij}\sigma_{s_j})^2$$

so that the standard deviation of the ith adjusted parameter is the root sum square (RSS) of the standard deviations due to data noise and a priori uncertainties and the standard deviations due to each unadjusted parameter.

5.0 MISSION STUDY CONFIGURATION

The ability of the "low-low" configuration to accurately recover geopotential fine structure of a given resolution (i.e. surface block size) depends on several factors:

a. satellite altitudes

b. satellite separation distances

c. SST data types

d. SST data rates

e. SST data noise

f. satellite state errors

g. a priori values of the surface densities

h. aliasing or orthogonality of the representation to the data type.

Other studies [(4), (9)] have investigated the GRAVSAT SST missions for factors (a-e) with somewhat positive results. In an attempt to establish the feasibility of local fine structure recovery using "low-low" SST data when factors (f-h) are considered we have restricted the surface density blocks to be 5° x 5° and the polar satellite orbits to be circular at 250 km altitude. Moreover, our investigation and that of Schwarz and Hajela have shown that SST range data is much less sensitive to fine structure detail than SST range-rate data. All studies presented in Section 6.0 utilize SST range-rate data.

The variation of the range-rate signal with satellite separation as the satellite pair passes over the *center 36* density blocks of Figure 3 (the remaining blocks being neglected) is illustrated in Figure 4-6, where each block has been approximated by 16 mass points. The values used for the surface block densities in Figure 3 are those obtained by Schwarz after removing the full 12th order gravity field. Figures 4-6 clearly show the trade-off between increasing signal strength and decreasing resolution of detail as the satellite separation is increased. The aliasing of the signal signature over these same blocks by adjacent blocks is illustrated in Figure 7, where now all 72 density blocks of Figure 3 have been included in the force model. Comparison with Figure 5 shows the signal signature over the central region to have only slight alteration, while the signal toward the edges of the 36 central blocks is considerably altered. This indicates that on a single pass, the effect of unaccounted-for density blocks severely aliases nearby blocks, but that the effect rapidly falls off with increasing distance. The short arc error analysis studies of Section 6.0 clearly

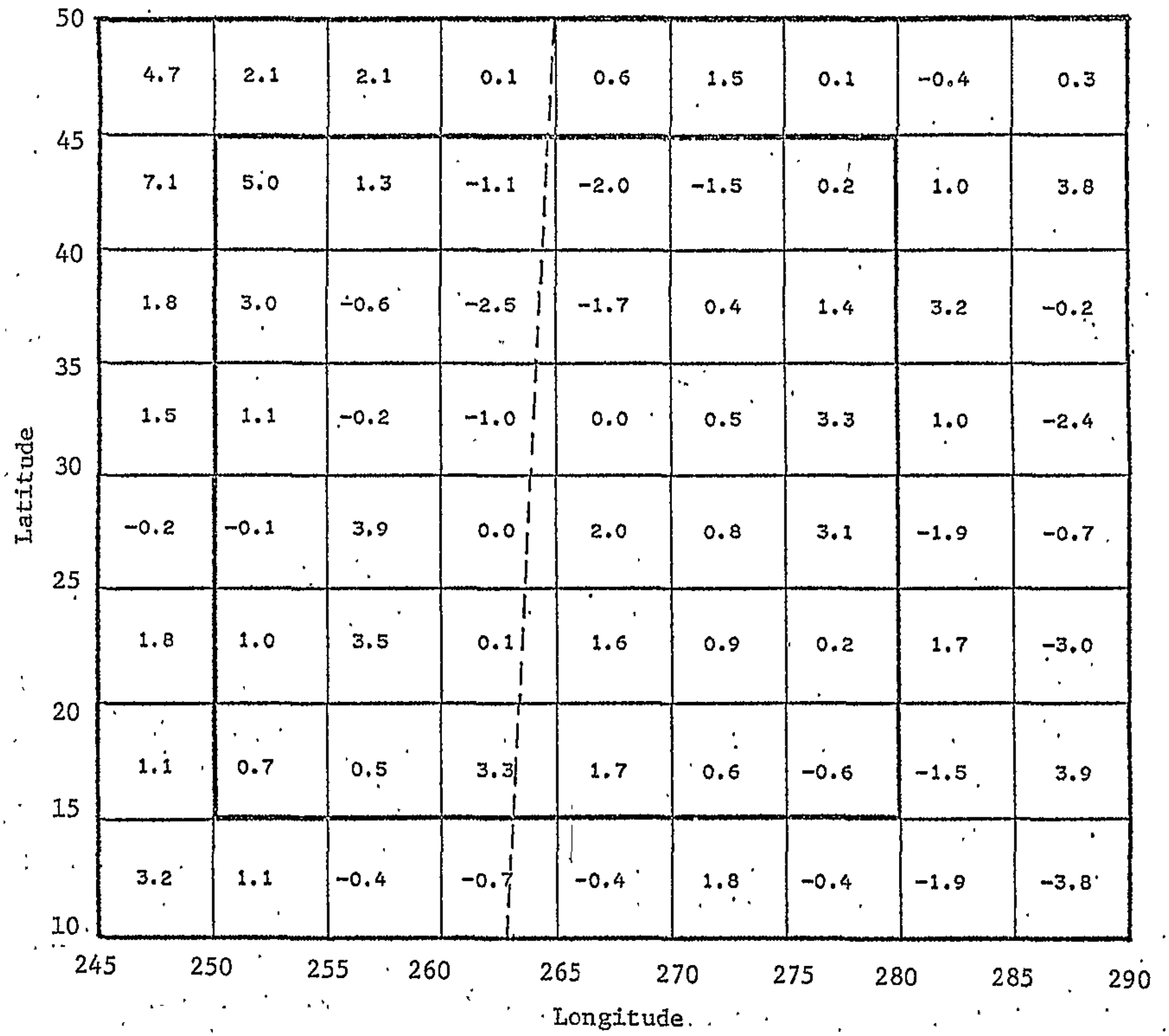

FIGURE 3. Mean surface density parameters for $5^{\circ} \times 5^{\circ}$ density blocks. These values were obtained by Schwarz by removing the 12th order gravity field. The dashed line represents the satellite ground track.

36 5° X 5° Surface Density Blocks
250 Km. Altitude
2° Satellite Separation
(16 Mass points per Block)

FIGURE 4

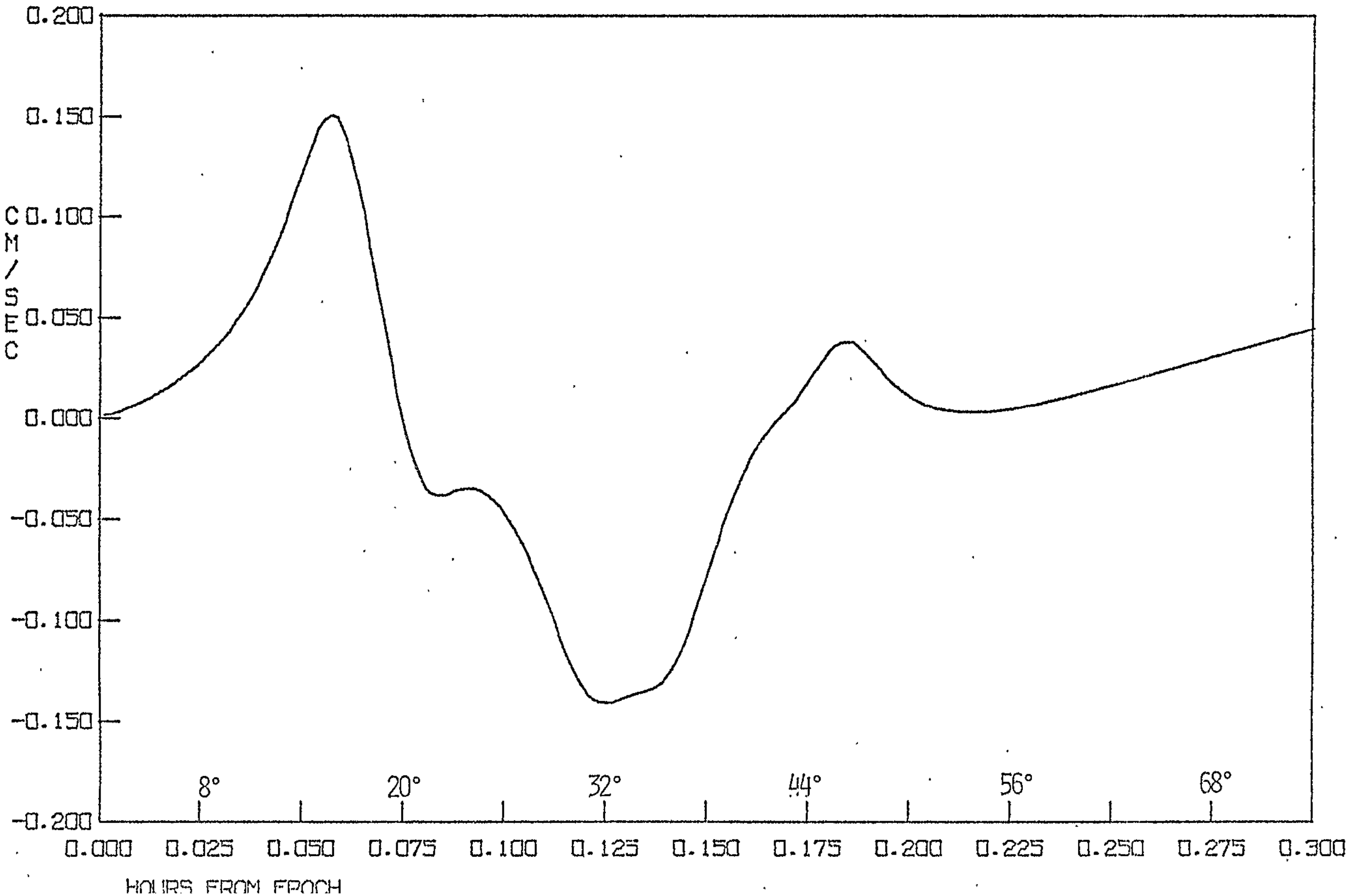

FIGURE 5

36 5° X 5° SURFACE DENSITY BLOCKS
250 KM. ALTITUDE
5° SATELLITE SEPARATION
(16 MASS POINTS PER BLOCK)

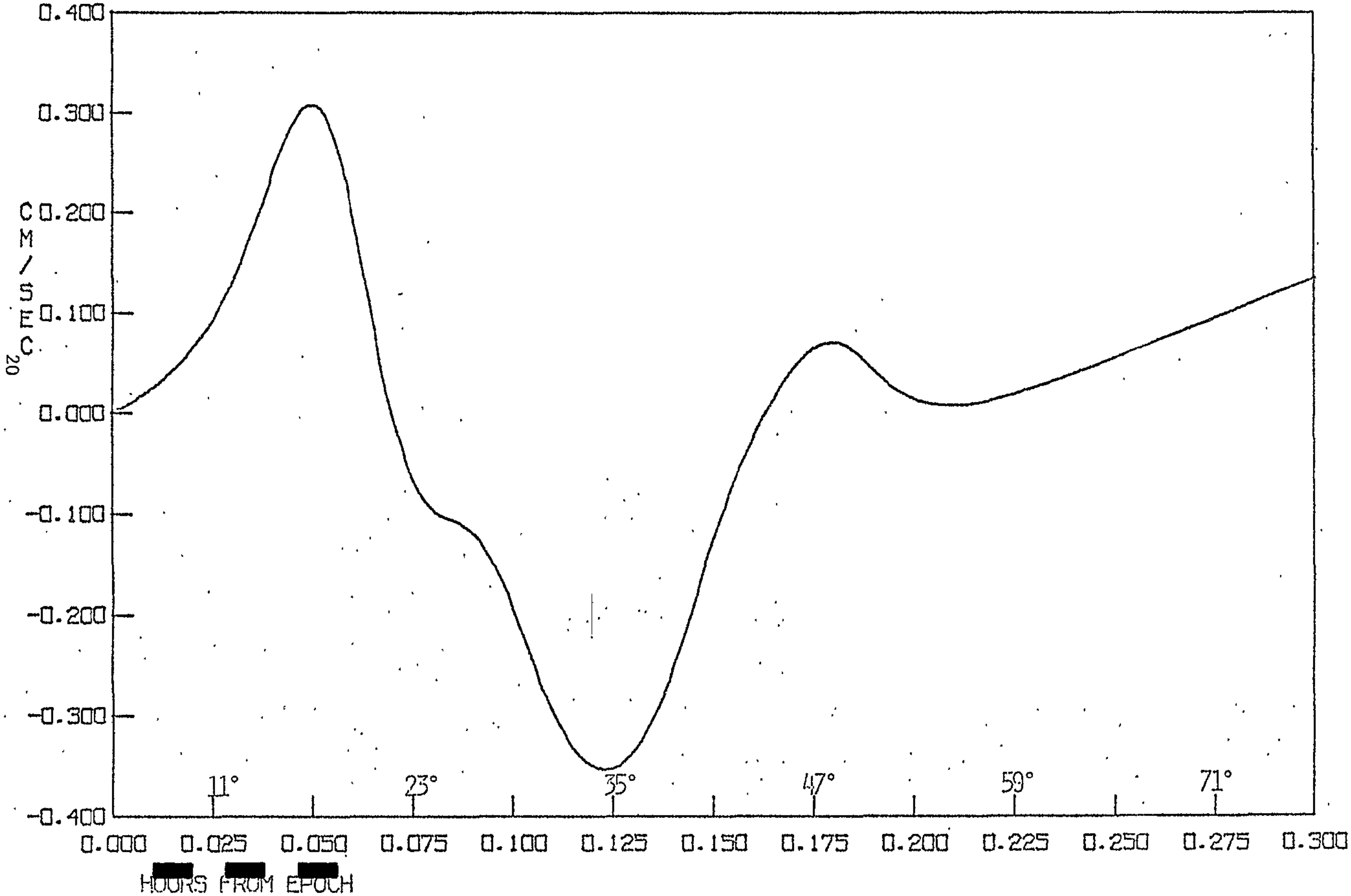

TRAJECTORY DIFFERENCES ***** RHODOT SST SLANT-RANGE RATE

FIGURE 6

36 5° X 5° SURFACE DENSITY BLOCKS
250 KM. ALTITUDE
7° SATELLITE SEPARATION
(16 MASS POINTS PER BLOCK)

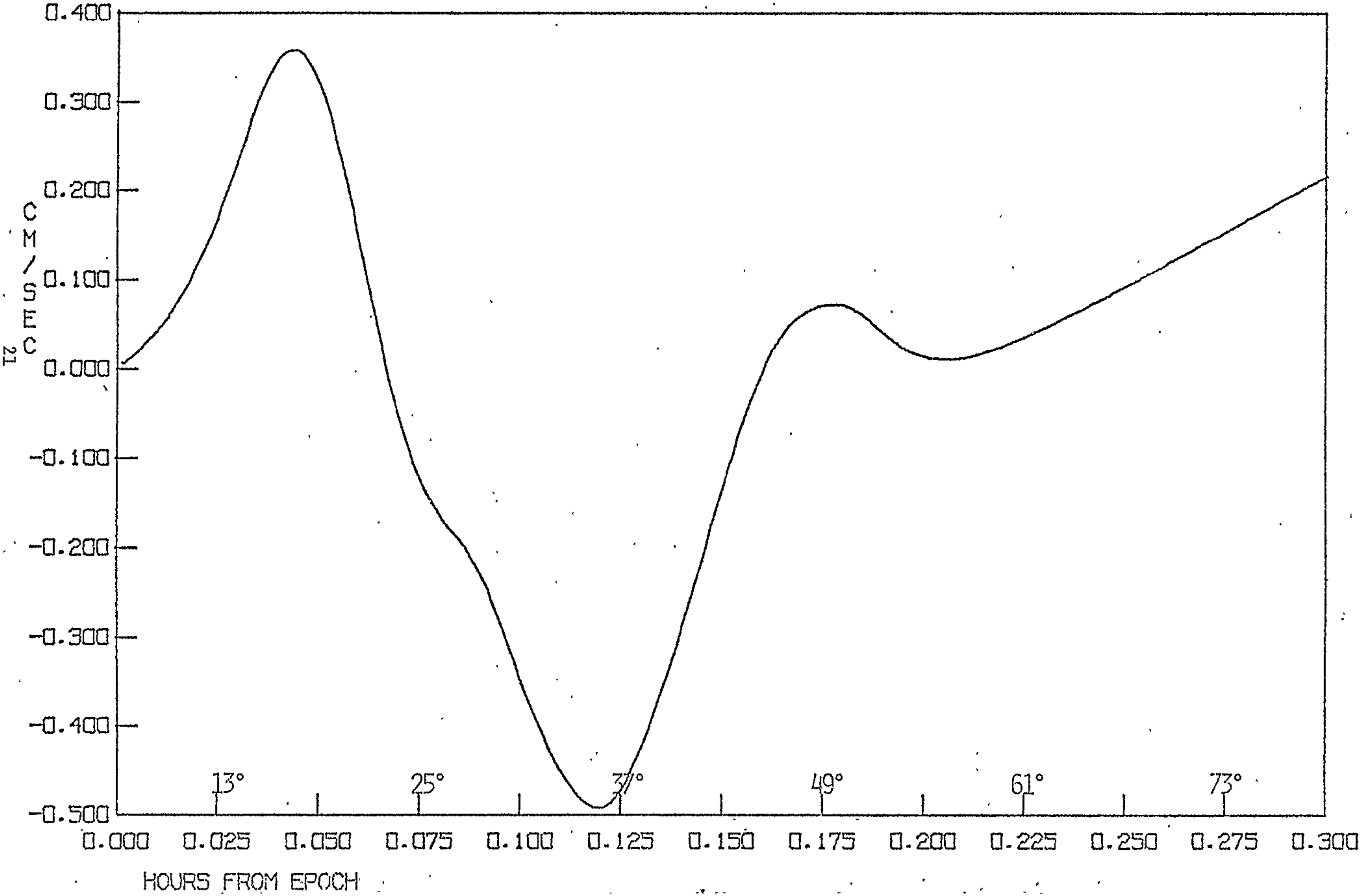

FIGURE 7

72 5° X 5° SURFACE DENSITY BLOCKS
250 KM. ALTITUDE
5° SATELLITE SEPARATION
(16 MASS POINTS PER BLOCK)

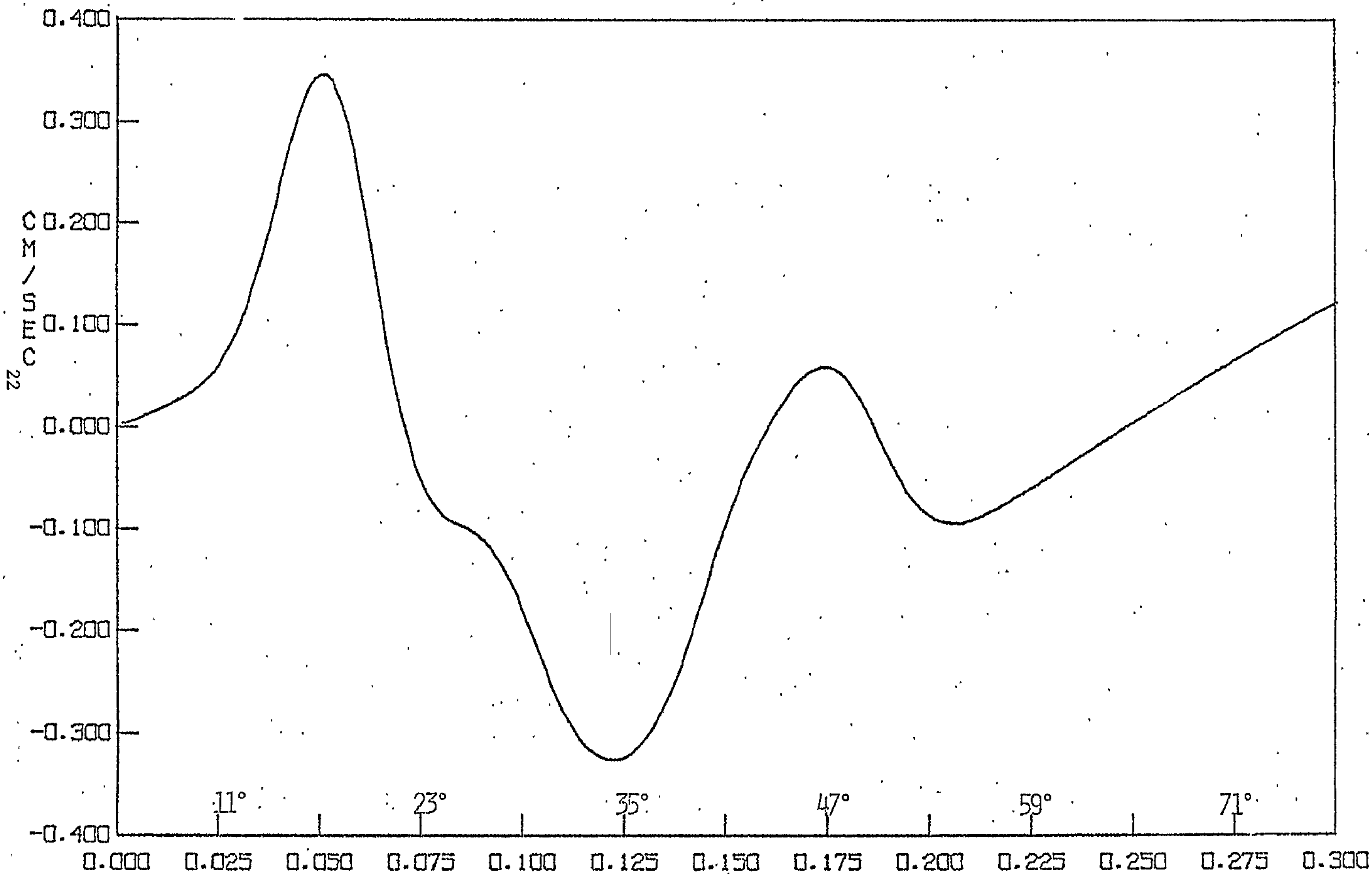

[redacted] HOURS FROM EPOCH

22

demonstrate this phenomena. The situation for long arcs is considerably different. The presence of unaccounted-for blocks perturbs the satellite orbit and the effect builds up through the dynamics over long arcs so that distant blocks can cause serious aliasing. This effect can be seen in comparing Figures 7 and 5 by noting that the two curves have different values and slopes at the end of the pass.

The long term perturbation of the orbit is clearly illustrated in Figure 8. Here the "low-low" configuration is in a circular equatorial two-body orbit at 250 km altitude, and perturbed through four orbital revolutions by a single 1 mgal 5° x 5° surface density block located on the equator. This shows that any unaccounted for block which perturbs the satellite orbit will alias the signal. The extent of the aliasing will be demonstrated in the long arc error analysis studies of Section 6.0.

Our computer analysis using ERODYN and GEOMAP in the estimation mode has shown that the optimum satellite separation is approximately 6°, or 700 km for the 5° x 5° surface blocks at 250 km altitude. Consequently, all error analysis results presented in this report will assume this separation. Moreover, our numerical studies have shown that for error analysis purposes the numerical approximation for the surface density force model evaluation offered by GEOMAP Option (2) (Section 3.0) with 9 mass points per block inside of a geocentric angle of 10° is of sufficient accuracy for the satellite configuration used and represented a substantial savings in computer time over Option (1).

The data rate assumed in this study is one observation every five seconds along the satellite path and four satellite passes per surface density block. This presents no problem for independent short arc solutions (less than one satellite period) since each arc normal matrix is generated separately and then concatenated, but for long arcs would require an excessive amount of computer run time to integrate the satellite orbits long enough to obtain the data coverage needed over a geographically localized set of density blocks. This problem was circumvented for the long arc simulations by slowing the rotational rate of the earth by a factor of 18 so that the satellite ground track precessed approximately 1.2° per revolution, producing the desired data coverage.

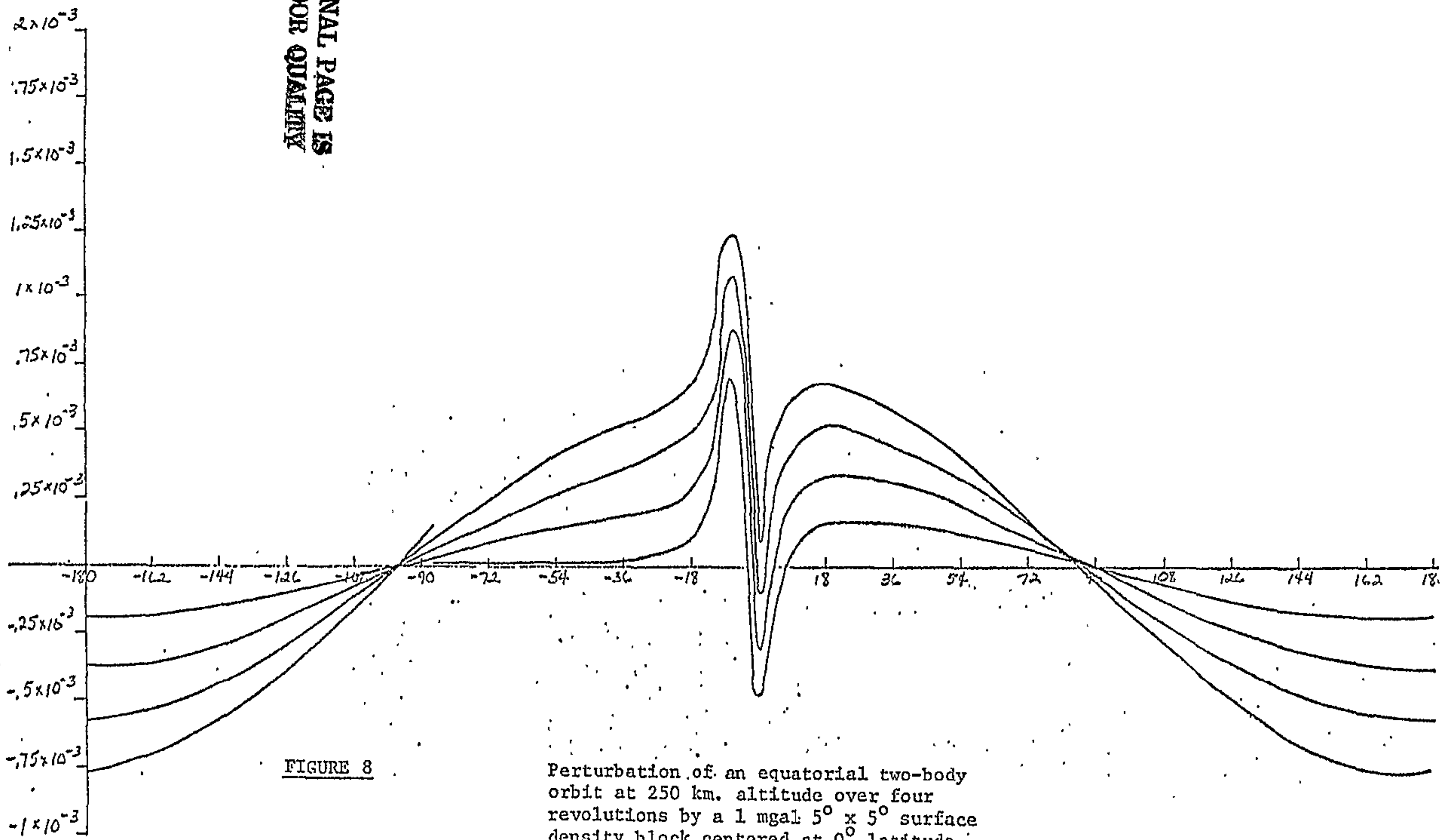

FIGURE 8

Perturbation of an equatorial two-body orbit at 250 km. altitude over four revolutions by a 1 mgal $5^{\circ} \times 5^{\circ}$ surface density block centered at 0° latitude, 0° longitude.

All data arcs consist of ascending satellite passes. This introduces some north-south asymmetry into the results, particularly for the short arcs, in that the variational equations for the block parameters are all propagated from zero initial conditions at epoch at the south edge of the set of blocks under consideration.northward along the data arc.

For final checkout of the GEOMAP/ERODYN system, the GEOMAP program was operated in the estimation mode for long arc *recoveries* of the center 36 blocks of Figure 3. Data was generated using only a two-body force model and the 36 perturbing density blocks. (This is, in fact, a global recovery in that no other blocks existed in the force model to alias the solution.) Recovery using perfect range-rate data (no noise), zero a priori density values, 10 mgal a priori surface density sigmas and perfect knowledge of the satellite states yielded three digits of accuracy (approx. .01 mgal) in the estimated surface densities, giving confidence as to the correctness of the GEOMAP software. Adding random noise with sigmas of .005 cm/sec and .05 cm/sec to the data resulted in estimated surface densities with 2 digits (approx. 0.1 mgal) and one digit (approx. 1.0 mgal) of accuracy, respectively. Error analysis results using ERODYN established consistency with these errors of the GEOMAP least squares parameter estimation.

6.0 ERROR ANALYSIS STUDY

From the example of aliasing in Section 5.0 it is clear that if a local set of density blocks is to be estimated the blocks near the edges will be badly corrupted by nearby unadjusted blocks, whereas blocks near the center of the set may be sufficiently far removed from the unadjusted blocks that their estimates may be acceptable. Thus, to estimate a given set of blocks it will be necessary to simultaneously estimate the set of interest plus a surrounding set of "buffer" blocks, whose estimates will be discarded due to aliasing. Moreover, the accuracy of the estimation of the center set of blocks of interest will depend on the region covered by observations in the estimation procedure. To determine the relationships between estimation accuracy and the estimation region, data region, data noise, a priori uncertainties in adjusted and unadjusted density blocks and a priori uncertainties in the satellite states we utilize the method of covariance error analysis outlined in Section 4.0. It must be stressed that in a covariance analysis the least squares estimation is postulated and not actually performed; only the covariance matrix for the estimator is calculated. Parameters in the adjust or "solve for" mode are assumed to be estimated in the postulated least squares adjustment, while parameters in the unadjust or "consider" mode are assumed to affect the functionality between the adjusted parameters and the observations but are not estimated in the postulated least squares adjustment. In several instances to be presented later the error analysis results somewhat strain intuition. However, it must be borne in mind that the error analysis problem treated here involves a large set of parameters, with many in the "consider" mode, and intuition can be misleading.

Two basic sets of 5° x 5° equal angular density blocks are used in the study:

1. 225 blocks arranged in a 15 block by 15 block square centered on the equator with data coverage over the center 25 blocks.
2. 289 blocks arranged in a 17 block by 17 block square centered on the equator with data coverage over the center 49 blocks.

The arrays of blocks were set to these large dimensions so that the results obtained for subsets of blocks in the interior would not be compromised by possible non-physical "edge" effects.

The placement of the block arrays on the equator minimizes any "area effect" due to decreasing block areas with increasing latitude. The data coverage over the twenty-five blocks is accomplished with 21 ground track passes, while the 49 block region required 31 passes. The data passes are symmetrically defined by the ground track of the midpoint between the two satellites. Figures 9 and 10 display the ground tracks over which data is taken for the two sets of blocks.

The total parameter set considered for the error analysis consists of six state parameters for each satellite for each arc plus the entire set of surface density parameters. The sensitivity matrix C, consisting of the partial derivatives of the observations with respect to the total parameter set, is evaluated along a nominal two body trajectory by setting the a priori values of all surface densities to zero. The resulting normal matrix is adequate for linear error analysis purposes and provides a substantial saving of computer time.

The error analysis results were generated under the following assumptions:

1. The two "low-low" satellites were configured in circular polar orbits at 250 km altitude with a 6° geocentric angle separation.
2. Satellite-to-satellite range-rate data was generated at 5 second intervals (15 data points per 5° block) with a noise of .05 cm/sec.
3. Data passes were at approximately 1.2° spacing, giving approximately four data passes per block.
4. All data was generated on ascending satellite passes.
5. A priori satellite epoch state errors reflect the orbital knowledge from other tracking means. No ground tracking data was included in the study.

The error analysis results are organized into four sets:

<u>SET I</u>. A single long data arc over the 225 block set. The twelve satellite state parameters are adjusted together with various subsets of blocks (Tables I.1 through I.6).

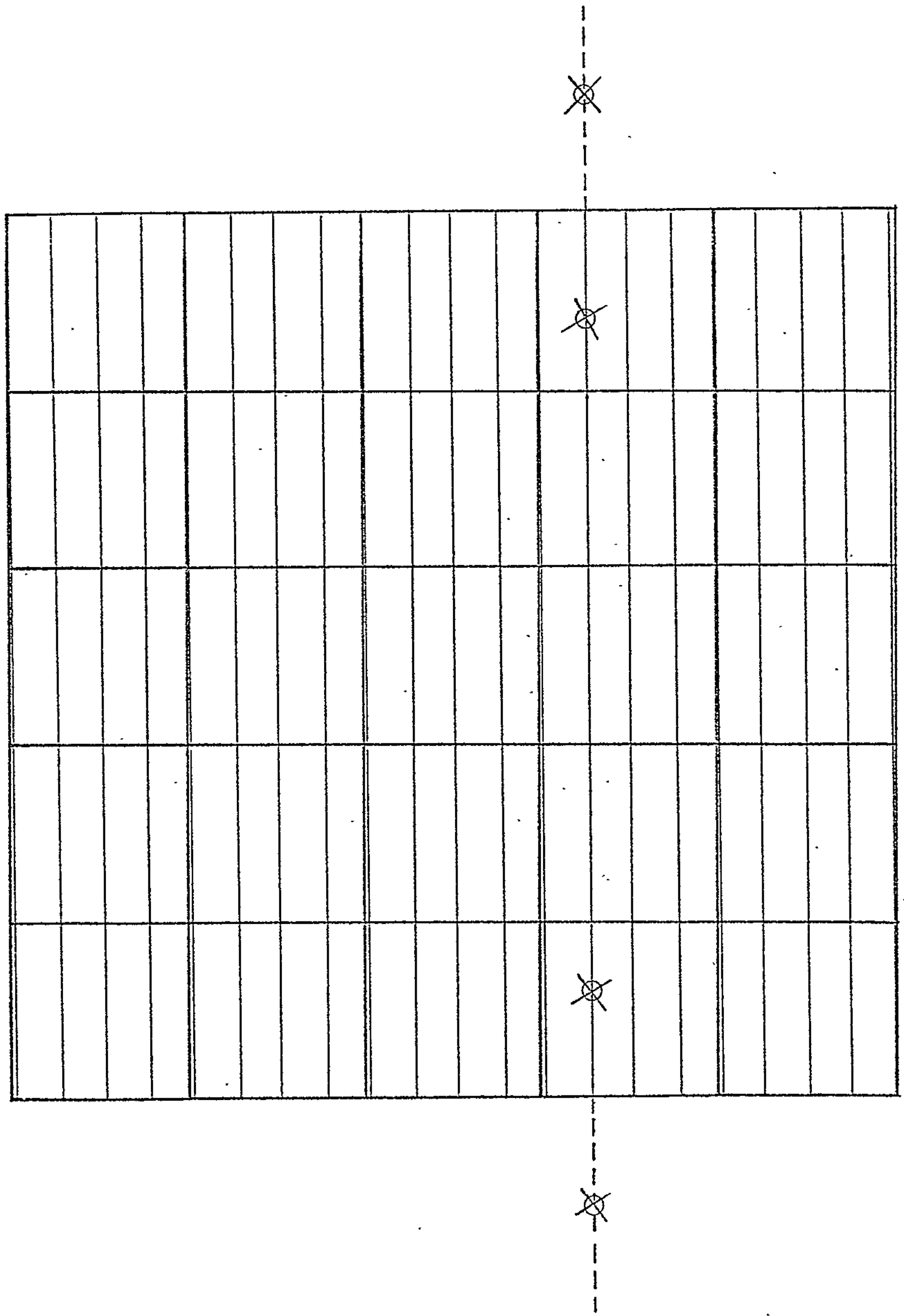

FIGURE 9   21 ascending short data arcs over 25 5° x 5° density blocks. Ground track spacing is approximately 1.2°.

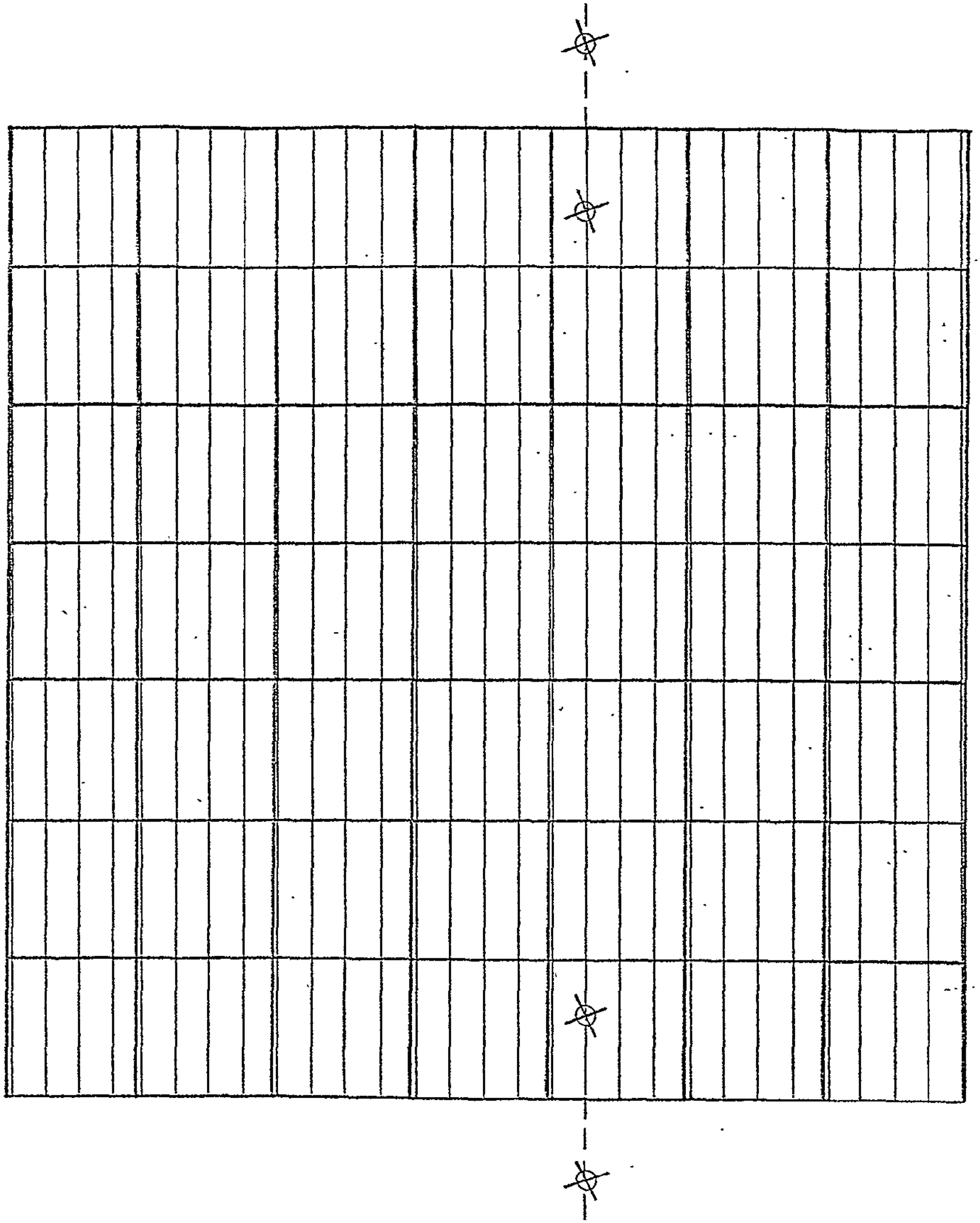

FIGURE 10 31 ascending short data arcs over 49 5° x 5° density blocks. Ground track spacing is approximately 1.2°.

SET II. Twenty-one short data arcs over the 225 block set. All 252 satellite state parameters are adjusted together with various subsets of blocks (Tables II.1 through II.20).

SET III. Thirty-one short data arcs over the 289 block set. All 372 satellite state parameters are adjusted together with various subsets of blocks (Tables III.1 through III.7).

SET IV. Both a single long data arc and twenty-one short arcs over the 225 block set. Aliasing is ignored and the satellite states are assumed perfectly known (Tables IV.1 through IV.4).

In the tables of solution sets I-IV displaying error sigmas, the dashed perimeter encloses the data region, while the solid perimeter encloses the set of adjusted density blocks. The two numbers within each adjusted block represent the total RSS error sigma for that block over the error sigma for that block due to aliasing by unadjusted blocks in milligals (mgal), i.e.

$$\sigma_{TOTAL} / \sigma_{ALIAS}$$

The error sigma due to data noise and a priori parameter uncertainties is then

$$\sigma_{NOISE} = \sqrt{\sigma^2_{TOTAL} - \sigma^2_{ALIAS}}$$

The numbers in unadjusted blocks represent the aliasing contribution of that block to the center adjusted block. The signs on these aliasing contributions reflect the influence of the sensitivity matrix $S = \frac{\partial \Delta X}{\partial \Delta S}$. In the tables of solution sets I-IV displaying correlations, the number within each adjusted block is the correlation of that adjusted block with the center adjusted block.

SET I:

The purpose of this set of studies is to analyze the effect of aliasing on long arc solutions. Long data arcs for this problem have not been treated by other investigators. As indicated in Section 5.0, to obtain reasonable computer run times, the rotational rate of the earth was slowed so that consecutive orbital ground tracks gave the proper spacing. This will certainly yield *optimistic* results in the error analysis since the dynamics will be correlated with a smaller number of unadjusted blocks than would be the case if the ground track passed

ORIGINAL PAGE IS
OF POOR QUALITY

over larger areas of the globe.

The normal matrix obtained for this study, as for all of Sets I-IV, displayed poor conditioning for the recovery of the satellite epoch state parameters. Other studies have avoided this problem by not estimating them or assuming them to be perfectly known (or, equivalently to have very small a priori sigmas). However, we have found that when the satellite epoch state parameters are placed in the unadjust mode with sigmas as small as .001 meters/.001 meters/sec for the positions and velocities, respectively (these numbers were chosen for convenience, the requirement being only that they be small), their aliasing error completely swamps the estimation of the density blocks. The satellite epoch states, unless perfectly known, must therefore be estimated along with the density blocks.

As could be guessed from the relative range-rate data type, the normal matrix is poorly conditioned for recovery of radial and cross track epoch state components, but is well conditioned for the recovery of along track epoch velocity components. In solution sets II and III this will be pursued by properly transforming sigma inputs in an HCL (radial, cross track, along track) coordinate system into a non-diagonal submatrix of the a priori covariance matrix. Otherwise all sigmas will be in cartesian coordinates in the diagonal a priori covariance matrix. In this solution set we set the epoch cartesian component sigmas to .001 meters and .001 meters/sec for position and velocity to give strong diagonality to the matrix

$$(A^T W A + P_A^{-1})$$

to avoid the numerical difficulties in inversion.

An estimation region which is exactly coincident with the data region (no buffer layer) is displayed in Table I.1. The a priori sigmas of the density blocks are 1 mgal. The recovery is seen to be very poor, with the a posteriori sigmas along the boundary larger than the a priori value of 1 mgal. The errors are dominated by the aliasing contribution with the along track (N-S) being more severe than cross track (E-W) since the satellite orbits do not pass over the blocks outside of the longitude interval defined by the data region. An important point is the slowness with which the aliasing contribution decreases in the N-S direction.

The effect of adding a single "buffer layer" is shown in Table I.2. The total error in the center of the estimated region decreased, but the aliasing error is still the dominant effect, showing a slow decrease with distance in the (N-S) direction. Table I.3 displays the effect of adding two buffer layers. Only a slight improvement is obtained, with the (N-S) aliasing still dominating the estimation accuracy. The correlations for the adjusted sets in Table I.1 and I.2 are displayed in Tables I.4 and I.5. The high correlations along track (N-S) reflect the fact that the relative range-rate data type is oriented along the satellite orbit.

The implication of these results is that if there were blocks distributed over the globe, any block which the satellite pair passed over could alias the adjusted blocks. Table I.6 clearly illustrates this fact. Here a band of 5°x 5° blocks completely encircles the globe passing through the poles. The data arc here consisted of a single long arc of 4 orbital revolutions with the earth slowed to give the proper data spacing. Again we see that the aliasing dominates the error of adjusted blocks. As before we see the aliasing contribution of the unadjusted blocks falling off very slowly, then increasing to a maximum on the opposite side of the earth.

This shows the low-low SST data type is unacceptable, due to severe aliasing, for recovery of localized density blocks for long arcs which pass over unadjusted blocks.

							-.18							
							-.20							
							-.22							
							-.25							
							-.30							
					1.22 1.20	.99 .97	.84 .82	.94 .92	1.24 1.24					
					.99 .99	.64 .62	.59 .58	.61 .60	.96 .95					
.02	.02	.02	.001	-.1	1.04 1.04	.82 .81	.82 .81	.82 .81	1.04 1.03	-.1	.001	.02	.02	.02
					.94 .94	.61 .60	.58 .56	.63 .62	.97 .97					
					1.23 1.23	.95 .93	.82 .80	1.00 .99	1.20 1.19					
							-.30							
							-.25							
							-.22							
							-.20							
							-.18							

TABLE I.1 A Posteriori Density Sigmas, One Long Data Arc (Data Noise = .05 cm/sec)

Adjusted parameters and a priori sigmas: 25 density blocks, σ = 1 mgal

Satellite States, σ_{POS} = .001

σ_{VEL} = .001

Unadjusted parameters and uncertainties: 200 density blocks, σ = 1 mgal

							-.14							
							-.15							
							-.16							
							-.14							
				.83 .57	.74 .47	.79 .48	.73 .46	.71 .43	.73 .45	.86 .56				
				.55 .44	.49 .36	.48 .35	.48 .35	.48 .35	.49 .36	.53 .40				
				.58 .53	.51 .45	.50 .45	.50 .45	.50 .46	.51 .46	.56 .51				
.01	.02	.02	.03	.58 .59	.50 .47	.49 .46	.49 .46	.49 .46	.50 .47	.58 .54	.03	.02	.02	.01
				.56 .50	.50 .45	.50 .45	.50 .45	.50 .45	.50 .44	.57 .52				
				.52 .39	.48 .34	.47 .33	.47 .33	.47 .33	.47 .33	.53 .41				
				.90 .63	.73 .46	.71 .43	.72 .46	.73 .46	.72 .45	.81 .56				
							-.14							
							-.16							
							-.15							
							-.14							

TABLE I.2 A Posteriori Density Sigmas, One Long Data Arc (Data Noise = .05 cm/sec)

Adjusted parameters and a priori sigmas: 49 density blocks, σ = 1 mgal

Satellite States, σ_{POS} = .001

σ_{VEL} = .001

Unadjusted parameters and uncertainties: 176 density blocks, σ = 1 mgal

							-.110							
							-.119							
							-.122							
			.995 .092	.944 .254	.920 .328	.915 .373	.914 .388	.911 .381	.910 .339	.937 .307	.992 .119			
			.975 .098	.740 .271	.647 .211	.646 .217	.640 .211	.636 .207	.648 .216	.755 .274	.977 .146			
			.957 .096	.498 .258	.447 .240	.437 .240	.436 .241	.437 .244	.450 .252	.496 .279	.964 .120			
			.935 .142	.482 .297	.428 .301	.421 .301	.420 .301	.422 .303	.431 .308	.478 .312	.941 .127			
.009	.011	.015	.935 .156	.478 .315	.424 .329	.415 .326	.413 .326	.415 .327	.423 .329	.478 .317	.938 .144	.016	.012	.010
			.938 .138	.473 .297	.426 .304	.419 .301	.417 .300	.417 .300	.421 .298	.477 .291	.937 .142			
			.963 .129	.491 .253	.440 .243	.431 .239	.430 .238	.431 .237	.433 .229	.484 .244	.958 .116			
			.979 .159	.778 .271	.650 .206	.636 .202	.640 .204	.641 .205	.639 .191	.711 .217	.966 .119			
			.994 .133	.947 .320	.925 .340	.916 .376	.914 .376	.912 .356	.900 .283	.800 .305	.979 .118			
							-.126							
							-.123							
							-.116							

TABLE I.3 A Posteriori Density Sigmas, One Long Data Arc (Data Noise = .05 cm/sec)

Adjusted parameters and a priori sigmas: 81 density blocks, σ = 1 mgal

Satellite States, σ_{POS} = .001

σ_{VEL} = .001

Unadjusted parameters and uncertainties: 144 density blocks, σ = 1 mgal

					-.08	.27	.77	.31	-.09					
					.30	-.1	.66	-.06	.30					
					.23	.03	1	.03	.22					
					.28	-.06	.64	-.1	.27					
					-.13	.30	.76	.25	-.13					

TABLE I.4 Correlations of Adjusted Blocks with Center Block. One Long Data Arc (Data Noise - .05 cm/sec)

Adjusted parameters and a priori sigmas: 25 density blocks, $\sigma = 1$ mgal

Satellite States, $\sigma_{POS} = .001$

$\sigma_{VEL} = .001$

Unadjusted parameters and uncertainties: 200 density blocks, $\sigma = 1$ mgal

.016	.024	.114	.28	.21	.05	.04
.16	.14	.03	.67	.12	.19	.16
.16	.19	-.005	.84	.041	.20	.16
.15	.23	-.08	1	-.07	.23	.15
.14	.19	.02	.84	-.02	.17	.14
.12	.16	.08	.65	-.002	.11	.12
-.005	.03	.19	.27	.11	.03	.02

TABLE I.5 Correlations of Adjusted Blocks with Center Block, One Long Data Arc (Data Noise - .05 cm/sec)

Adjusted parameters and a priori sigmas: 49 density blocks, σ = 1 mgal

Satellite States, σ_{POS} .001

σ_{VEL} .001

[redacted] Un[redacted]sted [redacted] para[redacted]ers [redacted] un[redacted]ain[redacted]: [redacted] de[redacted]y b[redacted]ks, [redacted] 1 [redacted]

.18	.18
.18	.19
.18	.18
.17	.18
.15	.17
.14	.16
.13	.15
.11	.14
.09	.12
.08	.11
.07	.09
.05	.07
.04	.06
.03	.04
.01	.03
.005	.02
0	.007
0	.001

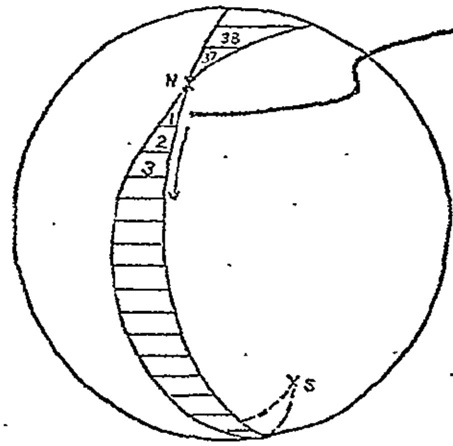

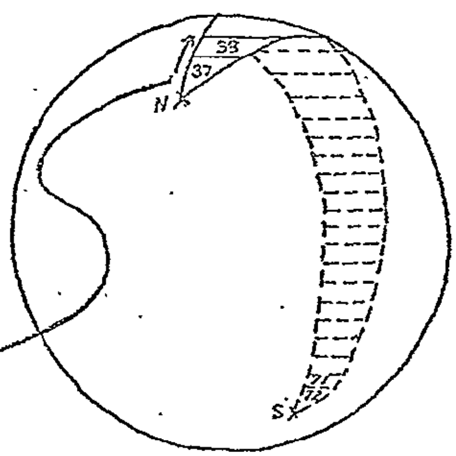

0	0
0	−.007
−.006	−.02
−.01	−.03
−.03	−.04
−.04	−.06
−.06	−.07
−.07	−.09
−.09	−.11
−.10	−.12
−.12	−.14
−.13	−.15
−.14	−.18
−.16	−.21
−.13	−.15
1.04 .81	1.05 .82
.86 .82	.83 .80
.95 .92	.94 .91

TABLE I.6

A Posteriori Density Sigmas One Long Data Arc (Polar Orbit over 4 revolutions)

Adjusted parameters and a priori sigmas: 6 density blocks, σ = 1 mgal

Satellite States σ_{POS} = .001

σ_{VEL} = .001

NOTE: Aliasing errors are with respect to adjusted block marked by pointer.

SET II:

Solution Set II consists of 21 independent short data arcs over the 25 center blocks. All results display the N-S asymmetry discussed in Section 5.0 due to the use of only ascending arcs with epochs along the south edge of the data region. This results in shifting the smallest error sigmas from the center of the adjusted set of blocks toward the south boundary in several cases. However, the center block remains the main focus of attention in these comparative studies for quantitative aliasing contributions.

Tables II.1–II.3 are to be compared directly with I.1–I.3. In both sets, the a priori error sigmas on the density blocks and the satellite states were 1 mgal and .001 m/.001 m/s (virtually no error, .001 chosen for convenience), respectively. The important point to note is that the aliasing error is no longer the dominating error source, as the aliasing contribution of unadjusted blocks decreases rapidly with distance from the adjusted set. Moreover, the additive "buffer layers" of Tables II.2 and II.3 show dramatic decreases in the aliasing error contribution to the center block. The dominant error source is now the "noise plus a priori" contribution arising from

$$(A^T WA + P_A^{-1})^{-1} \quad .$$

The complicated dependencies of the components of total error on the *a priori sigmas* for the satellite epoch state and the density blocks are investigated in Tables II.5 through II.20.

Tables II.5, II.6 and II.7 where the a priori errors on the satellite epoch states are systematically increased are designed to be compared with Table II.1. Table II.5 displays the surprising result that an increase in the satellite epoch state a priori to σ = .002 (meters and meters/sec) results in a *decrease* in both the total error and the aliasing contribution to the center adjusted block. It must be noted, however, that there are increases in error to some of the adjusted blocks and that the total error to *all* adjusted parameters (satellite epoch states plus the 25 adjusted density blocks) increases. Table II.6, with an increase in the a priori epoch sigmas to σ = .01 shows an *increase* in the total error sigma of the center block (but a decrease in the alias error) while some of the blocks in the northern sector again show a decrease. As indicated previously, the covariance matrix is poorly conditioned for the estimation of the radial and cross track components of the satellite states, as would be expected for the SST range-rate data. The inversion of the normal matrix plus the inverse a priori covariance matrix broke down due to loss of significant digits when the a priori velocity sigmas were increased beyond σ = .01 m/s for the Cartesian components. In an attempt to utilize realistic sigmas, the option to input satellite epoch sigmas in a radial, cross track, along track (denoted HCL) coordinate system was implemented. The maximum satellite state error sigmas permissible before inversion failure (with triple precision arithmetic for the inversion algorithm) was determined to be 10 meters in the position components and .01 meters/sec in the radial and cross track velocity components. As would be expected for the data type, the along track velocity showed a high recoverability, with error sigmas up to 100 meters/sec showing no inversion difficulties and the a posteriori estimated error sigma less than 1 meter/sec. Tables II.7 and II.8 show the effect on the adjusted blocks of increasing the along track a priori velocity sigma values to 2 meters/sec and 5 meters/sec, respectively, with 10 meters in position and .01 meters/sec in the radial and cross track velocities.

The effect of the a priori sigmas of the density blocks is investigated in Tables II.9-II.11 where the density block sigmas are set to 50 mgal and the estimation configurations of Table II.1 through II.3 are repeated. This set of solutions clearly demonstrates the importance of adding buffer layers. When the adjusted region covers the data region and one buffer layer around the data region the aliasing due to the large uncertainties in the unadjusted blocks is the dominating effect. The addition of two buffer layers in Table II.11, however, drastically reduces both the total error of the interior blocks and the fraction of the total error due to aliasing. It should be noted in comparing Tables II.1 and II.9 that although the estimation strategy of adjusting all blocks in the data region with no buffer layers is a poor one, it does show some improvement with an assumed a priori knowledge of all density blocks to 1 mgal. The assumption of a 50 mgal a priori uncertainty in the density blocks, however, results in a worsened solution.

The effect of systematically increasing the a priori surface density sigmas for a one layer buffer zone and satellite epoch state sigmas of 10 meters in position, .01 meters/sec in radial and cross track velocities, and 2 meters/sec in along track velocity is presented in Tables II.12 through II.17. The case of

100 mgal a priori uncertainty of Table II.15 shows the aliasing error again becoming the dominant effect. Table II.16 shows the effect of having good a priori knowledge of the adjusted blocks (σ = 1 mgal) and little a priori knowledge of the unadjusted blocks (σ = 50 mgal). The recovery is destroyed by the dominating alias error. The opposite extreme of poor a priori knowledge of the adjusted set (50 mgal) and good a priori knowledge of the unadjusted set (σ = 1 mgal) is shown in Table II.17. As would be suspected, this recovery suffers little from aliasing errors. The case for two buffer layers and a priori surface density sigmas of 50 mgal is shown in Table II.18. Comparing this result with the single buffer layer of Table II.14 shows a much less dramatic improvement in estimated accuracy for the adjusted blocks than the similar cases with small a priori sigmas on the satellite states (Tables II.10 and II.11), indicating the importance of some amount of a priori knowledge.

The effect of reduced data noise is displayed in Tables II.19 and II.20 where the noise sigma is set to .01 cm/sec, while the satellite state sigmas are kept small (.001) and the surface density block sigmas are set at 1 mgal. These results are to be compared with Tables II.2 and II.3 where the data noise is .05 cm/sec. The total error decreased in both cases II.19 and II.20, while the aliasing contribution increased slightly. The dominating error source in these cases is the a priori uncertainties in the adjusted parameters.

							.005							
							.009							
							.02							
							.06							
							.17							
					.81/.76	.67/.59	.67/.58	.70/.62	.88/.83					
					.81/.74	.65/.52	.65/.52	.69/.58	.92/.86					
-.001	-.002	-.003	-.008	-.04	.73/.63	.57/.37	.57/.39	.60/.44	.84/.76	-.06	-.01	-.003	-.002	-.001
					.61/.51	.45/.24	.44/.23	.46/.28	.67/.59					
					.55/.48	.42/.30	.41/.28	.44/.33	.62/.57					
							-.27							
							-.03							
							0							
							.002							
							.001							

TABLE II.1 A Posteriori Density Sigmas. 21 Short Data Arcs (Data Noise = .05 cm/sec)

Adjusted parameters and a priori sigmas: 25 density blocks, σ = 1 mgal

Satellite States, σ_{POS} = .001

σ_{VEL} = .001

Unadjusted parameters and uncertainties: 200 density blocks, σ = 1 mgal

							.005							
							.009							
							.02							
							.04							
				.91 .09	.78 .08	.77 .06	.76 .07	.76 .08	.78 .09	.87 .12				
				.69 .19	.54 .18	.51 .18	.50 .18	.51 .19	.52 .19	.59 .22				
				.65 .16	.52 .12	.50 .13	.50 .12	.50 .12	.51 .13	.57 .20				
-.001	-.002	-.003	-.005	.64 .14	.50 .11	.48 .10	.48 .09	.48 .10	.49 .11	.56 .18	-.004	-.003	-.002	-.001
				.63 .15	.43 .09	.39 .07	.39 .07	.39 .07	.42 .09	.52 .19				
				.67 .15	.41 .14	.35 .12	.35 .12	.35 .12	.39 .13	.51 .21				
				.92 .10	.71 .16	.68 .13	.69 .14	.69 .14	.70 .15	.84 .14				
							-.04							
							-.005							
							-.0005							
							.00008							

TABLE II.2 A Posteriori Density Sigmas
21 Short Data Arcs (Date Noise - .05 cm/sec)
Adjusted Parameter and a priori sigmas: 49 density blocks, σ = 1 mgal

Satellite States, σ_{POS} = .001

σ_{VEL} = .001

Unadjusted Parameters and uncertainties: 176 density blocks. σ = 1 mgal

							.004							
							.007							
							.01							
			.99 .007	.98 .03	.95 .06	.95 .06	.94 .06	.94 .06	.94 .06	.97 .04	.99 .01			
			.99 .006	.91 .03	.78 .03	.77 .01	.76 .02	.76 .02	.78 .03	.87 .04	.97 .009			
			.99 .02	.68 .05	.53 .05	.50 .05	.50 .05	.50 .05	.52 .05	.57 .06	.98 .02			
			.99 .02	.65 .04	.52 .04	.50 .04	.50 .04	.51 .04	.57 .04	.98 .05	.99 .03			
-.001	-.002	-.003	.99 .02	.64 .04	.50 .04	.48 .03	.48 .03	.48 .03	.49 .04	.56 .05	.98 .02	-.002	-.002	-.001
			.99 .02	.63 .05	.43 .04	.40 .03	.40 .03	.40 .03	.41 .04	.51 .06	.98 .02			
			.99 .01	.67 .05	.40 .05	.35 .04	.35 .04	.35 .04	.38 .05	.51 .06	.78 .02			
			.99 .005	.92 .02	.71 .05	.67 .04	.68 .04	.69 .04	.69 .05	.84 .04	.99 .007			
			.99 .003	.97 .01	.96 .03	.96 .03	.97 .03	.97 .03	.96 .03	.98 .02	.99 .005			
							-.003							
							-.0008							
							.0003							

TABLE II.3 A Posteriori Density Sigmas
21 Short Data Arcs (Data Noise - .05 cm/sec)
Adjusted parameters and a priori sigmas: 81 density blocks, σ = 1 mgal

Satellite States, σ_{POS} = .001

σ_{VEL} = .001

Unadjusted parameters and uncertainties: 144 density blocks, σ = 1 mgal

ORIGINAL PAGE IS OF POOR QUALITY

			0	.003	.03	.06	.06	.07	.03	.003	0			
			-.005	-.019	-.029	.147	.11	.149	-.035	-.021	-.005			
			-.005	-.005	-.085	-.054	.70	-.059	-.081	-.011	-.007			
			-.007	-.008	-.06	-.192	.86	-.194	-.06	-.015	-.006			
			-.009	-.04	-.014	-.31	1	-.31	-.019	-.030	-.005			
			-.006	-.004	-.019	-.27	.81	-.27	-.02	-.005	-.006			
			-.004	.004	-.007	-.135	.47	-.142	-.004	.001	-.006			
			-.003	-.002	.047	.046	-.30	.03	.047	.001	-.003			
			-.001	.003	.015	-.013	-.07	-.017	.014	.005	0			

TABLE II.4 Correlations of Adjusted Blocks with Center Block
21 Short Data Arcs (Data Noise = .05 cm/sec)
Adjusted parameters and a priori sigmas: 81 density blocks, σ = 1 mgal

Satellite States, σ_{POS} = .001

σ_{VEL} = .001

Unadjusted parameters and uncertainties: 144 density blocks, σ = 1 mgal

							.004							
							.007							
							.01							
							.02							
							.07							
					.73 / .64	.62 / .51	.61 / .49	.65 / .54	.79 / .72					
					.70 / .57	.58 / .40	.58 / .39	.63 / .46	.82 / .72					
-.002	-.003	-.005	-.01	-.05	.66 / .48	.54 / .27	.52 / .23	.56 / .32	.79 / .65	-.07	-.02	-.005	-.003	-.002
					.62 / .48	.47 / .27	.47 / .23	.50 / .30	.68 / .56					
					.61 / .52	.50 / .37	.49 / .36	.53 / .41	.66 / .58					
							-.14							
							-.03							
							-.001							
							.0001							
							.0008							

TABLE II.5 A Posteriori Density Sigmas
21 Short Data Arcs (Data Noise = .05 cm/sec)
Adjusted parameters and a priori sigmas: 25 density blocks, σ = 1 mgal

Satellite States, σ_{POS} = .002

σ_{VEL} = .002

Unadjusted parameters and uncertainties: 200 density blocks, σ = 1 mgal

							-.0005							
							-.002							
							-.006							
							-.03							
							.009							
					.68 .55	.59 .43	.57 .41	.62 .48	.74 .62					
					.66 .47	.57 .30	.56 .30	.61 .38	.79 .64					
-.0006	-.001	-.003	-.01	-.05	.67 .42	.56 .18	.55 .18	.57 .23	.82 .65	-.08	-.02	-.004	-.001	-.0006
					.68 .52	.55 .31	.54 .29	.57 .34	.75 .60					
					.68 .57	.57 .43	.56 .41	.60 .48	.72 .62					
							-.01							
							-.03							
							-.05							
							-.001							
							-.0004							

TABLE II.6 A Posteriori Density Sigmas
21 Short Data Arcs (Data Noise = .05 cm/sec)
Adjusted Parameters and a priori sigmas: 25 density blocks, σ = 1 mgal

Satellite States, σ_{POS} = .01

σ_{VEL} = .01

Unadjusted parameters and uncertainties: 200 density blocks, σ = 1 mgal

							-.001							
							-.002							
							-.008							
							-.04							
							.004							
					.68 .38	.64 .30	.64 .29	.66 .35	.70 .42					
					.69 .44	.60 .22	.60 .23	.62 .30	.76 .55					
-.0003	-.0008	-.002	-.01	-.05	.67 .42	.56 .19	.56 .18	.58 .22	.83 .65	-.08	-.02	-.004	-.001	-.0004
					.66 .40	.59 .34	.59 .22	.61 .26	.80 .61					
					.70 .42	.64 .31	.63 .29	.64 .31	.67 .48					
							-.003							
							-.03							
							-.006							
							-.002							
							-.0007							

TABLE II.7 A Posteriori Density Sigmas
21 Short Data Arcs (Data Noise = .05 cm/sec)
Adjusted parameters and a priori sigmas: 25 density blocks, σ = 1 mgal

Satellite States, σ_{POS} = 10

σ_{VEL} [HCL] = (.01, .01, 2)

Unadjusted parameters and uncertainties: 200 density blocks, σ = 1 mgal

							-.001							
							-.002							
							-.008							
							-.04							
							.004							
					.68 .38	.64 .30	.64 .30	.66 .35	.70 .42					
					.69 .43	.60 .22	.60 .23	.62 .30	.76 .55					
-.0003	-.0008	-.002	-.01	-.05	.67 .42	.56 .19	.56 .18	.58 .22	.83 .65	-.08	-.02	-.004	-.001	-.0004
					.66 .40	.60 .24	.59 .22	.61 .26	.80 .61					
					.70 .42	.64 .31	.63 .29	.64 .31	.67 .40					
							-.003							
							-.03							
							-.006							
							-.002							
							-.0007							

TABLE II.8 A Posteriori Density Sigmas
21 Short Data Arcs (Data Noise = .05 cm/sec)
Adjusted parameters and a priori sigmas: 25 density blocks, σ = 1 mgal

Satellite States σ_{POS} = 10

σ_{VEL} [HCL] = (.01, .01, 5)

Unadjusted Parameters and uncertainties: 200 density blocks, σ = 1 mgal

							.34							
							.63							
							1.5							
							5.9							
							33.9							
					57.6 57.6	63.5 63.5	64.9 64.9	67.6 67.6	62.1 62.1					
					66.7 66.7	76.9 76.9	80.3 80.3	85.2 85.2	76.7 76.7					
-.25	-.49	-1.2	-3.6	-13.3	65.7 65.7	75.7 75.7	79.2 79.2	84.3 84.3	76.2 76.2	-22.6	-6.4	-1.9	-.72	-.35
					48.4 48.4	53.6 53.6	56.1 56.1	58.3 58.2	52.3 52.3					
					28.4 28.4	24.5 24.5	25.5 25.5	26.0 26.0	31.0 31.0					
							-45.9							
							-5.5							
							-.16							
							.07							
							.05							

TABLE II.9 A Posteriori Density Sigmas
21 Short Data Arcs (Data Noise = .05 cm/sec)
Adjusted parameters and a priori sigmas: 25 density blocks, σ = 50 mgal

Satellite States, σ_{POS} = .001

σ_{VEL} = .001

Unadjusted parameters and uncertainties: 200 density blocks, σ = 50 mgal

ORIGINAL PAGE IS OF POOR QUALITY

							.42							
							1.0							
							3.4							
							19.1							
				44.6 43.5	30.2 29.3	36.2 35.8	37.0 36.6	37.0 35.6	33.7 32.9	42.9 42.1				
				44.0 43.4	29.1 28.3	37.2 36.8	38.2 37.8	38.1 37.6	34.7 33.7	44.9 44.3				
				41.4 40.8	26.1 25.1	34.7 34.3	35.9 35.4	35.7 35.0	32.6 31.6	43.4 42.9				
-.05	-.06	-.07	.01	34.8 34.2	28.5 20.6	28.5 28.5	30.0 29.5	29.7 29.1	27.6 26.6	37.3 36.8	-.03	-.11	-.10	-.07
				24.9 24.5	15.5 14.8	20.5 20.1	21.3 20.7	21.1 20.6	20.0 19.3	27.7 27.3				
				15.5 15.2	10.0 9.6	11.3 11.1	11.8 11.6	11.9 11.6	11.9 11.5	16.4 16.1				
				24.2 23.6	12.6 12.4	13.3 13.2	13.6 13.5	13.9 13.8	13.4 13.2	18.8 18.6				
							-18.9							
							-2.2							
							-.36							
							-.08							

TABLE II.10 A Posteriori Density Sigmas
21 Short Data Arcs (Data Noise - .05 cm/sec)
Adjusted parameters and a priori sigmas: 49 density blocks, σ = 50 mgal

Satellite States, σ_{POS} = .001

σ_{VEL} = .001

Unadjusted parameters and uncertainties: 176 density blocks, σ = 50 mgal

							.18							
							.35							
							.92							
			49.1 2.2	37.3 8.1	26.4 7.8	24.8 7.5	24.6 7.6	25.9 7.7	25.7 7.8	35.4 8.3	47.8 3.2			
			47.0 1.9	23.4 3.5	14.2 2.4	13.4 2.3	13.4 2.2	13.9 2.2	14.4 2.4	20.6 2.6	42.3 4.4			
			42.6 4.6	20.3 7.4	12.4 2.3	11.4 2.2	11.6 2.1	12.3 2.1	13.2 2.4	17.9 2.8	32.4 7.7			
			41.2 4.7	18.7 3.9	11.1 2.3	9.9 2.0	10.1 1.9	11.0 1.9	12.3 2.4	16.6 3.4	30.4 7.5			
−.05	−.06	−.09	41.8 4.3	17.5 4.3	9.6 2.2	8.3 1.9	8.5 1.8	9.3 1.8	10.8 2.3	15.3 3.7	30.3 7.0	−.13	−.08	−.06
			40.0 4.7	14.7 4.1	7.8 2.2	6.5 1.9	6.7 1.8	7.3 1.9	8.6 2.9	13.1 7.8	28.0 2.0			
			43.4 3.9	12.0 2.8	6.4 2.8	5.5 1.9	5.6 1.9	5.8 1.9	6.6 2.8	10.9 3.8	29.8 7.7			
			46.8 2.6	16.3 3.6	7.5 2.4	7.1 2.1	7.1 2.0	7.1 2.1	7.2 2.4	12.1 3.5	42.0 4.6			
			49.3 1.3	39.8 6.8	21.7 7.8	20.1 8.3	20.1 8.4	20.1 8.1	20.0 7.8	24.0 8.6	47.7 3.1			
							.23							
							.21							
							.09							

TABLE II.11 A Posteriori Density Sigmas
21 Short Data Arcs (Data Noise = .05 cm/sec)
Adjusted parameters and a priori sigmas: 81 density blocks, σ = 50 mgal

Satellite States σ_{POS} = .001

σ_{VEL} = .001

Unadjusted parameters and uncertainties: 144 density blocks, σ = 50 mgal

							-.0008							
							-.002							
							-.006							
							-.03							
				.96 .04	.85 .08	.85 .08	.84 .08	.83 .09	.84 .08	.94 .05				
				.79 .1	.63 .06	.61 .06	.61 .06	.61 .06	.62 .07	.71 .13				
				.72 .09	.59 .05	.57 .05	.57 .05	.57 .05	.58 .05	.64 .11				
-.0001	-.0003	-.0006	-.002	.67 .11	.56 .05	.54 .05	.54 .05	.54 .05	.54 .05	.60 .14	-.0004	-.0004	-.0002	-.0001
				.73 .08	.58 .05	.57 .04	.57 .04	.57 .04	.58 .05	.63 .12				
				.79 .1	.63 .07	.61 .07	.61 .07	.61 .07	.62 .07	.70 .14				
				.96 .04	.84 .08	.83 .09	.84 .08	.85 .07	.84 .09	.93 .06				
							-.03							
							-.005							
							-.002							
							-.0006							

TABLE II.12 A Posteriori Density Sigmas
21 Short Data Arcs (Data Noise = .05 cm/sec)
Adjusted parameters and a priori sigmas: 49 density blocks, σ = 1 mgal

Satellite States, σ = 10

σ_{VEL}[HCL] = (.01, .01, 2)

Unadjusted parameters and uncertainties: 176 density blocks, σ = 1 mgal

							-.01							
							-.03							
							-.13							
							-.9							
				9.8 5.8	7.7 4.7	7.8 5.7	7.8 5.9	7.9 5.9	7.6 5.2	9.2 6.3				
				8.3 4.2	6.8 2.6	6.9 3.4	6.9 3.5	6.9 3.5	6.9 2.8	8.1 4.7				
				7.9 3.1	6.8 1.1	6.8 1.5	6.8 1.5	6.8 1.5	6.8 1.3	7.8 3.4				
.001	.002	-.004	.008	7.6 2.5	6.8 .9	6.8 1.0	6.7 1.0	6.7 1.0	6.8 1.0	7.4 2.6	.09	.02	.004	.002
				7.8 3.3	6.8 1.6	6.8 2.2	6.8 2.3	6.7 2.3	6.8 1.8	7.7 3.7				
				8.2 4.5	6.9 3.2	7.1 4.2	7.1 4.3	7.1 4.3	6.9 3.4	8.1 5.2				
				10. 6.	7.8 5.3	8.1 6.4	8.0 6.4	8.0 6.3	7.7 5.6	9.2 6.9				
							-.26							
							-.04							
							.007							
							-.00004							

TABLE II.13 A Posteriori Density Sigmas
21 Short Data Arcs (Data Noise = .05 cm/sec)
Adjusted parameters and a priori sigma: 49 density blocks, σ = 15 mgal

Satellite States, σ_{POS} = 10

σ_{VEL} [HCL] = (.01, .01, 2)

Unadjusted parameters and uncertainties: 176 density blocks, σ = 15 mgal

							-.03							
							.06							
							.4							
							.3							
				32/28	24/21	26/24	27/25	27/25	25/23	31/27				
				28/20	21/15	22/17	22/17	22/18	21/16	27/21				
				25/13	20/12	20/12	19/12	19/12	20/11	24/12				
.06	.1	.06	.4	23/8	20/12	20/12	20/12	20/13	20/11	22/6	1.6	.3	.1	.06
				25/14	21/14	23/18	23/18	22/17	21/14	26/16				
				29/22	23/18	27/24	27/24	26/24	24/20	30/25				
				33/30	26/24	31/29	31/29	30/29	28/26	33/31				
							11							
							1.5							
							.6							
							.16							

TABLE II.14 A Posteriori Density Sigmas
21 Short Data Arcs (Data Noise = .05 cm/sec)
Adjusted parameters and a priori sigmas: 49 density blocks, = 50 mgal

Satellite States, $\sigma_{\vec{POS}}$ = 10

σ_{VEL}[HCL] = (.01, .01. 2)

Unadjusted parameters and uncertainties: 176 density blocks, σ = 50 mgal

							-.059							
							.291							
							1.78							
							2.87							
				66.2/61.2	55.2/53.2	57.3/55.7	57.3/55.9	57.4/56.2	55.3/53.6	67.4/63.8				
				56.8/46.1	50.7/47.3	49.5/46.3	47.9/45.0	47.9/45.3	47.8/44.4	62.7/55.7				
				48.8/30.0	49.6/44.9	47.0/42.4	43.6/39.2	43.2/39.3	44.3/39.3	54.0/42.4				
.204	.361	.215	1.28	44.5/20.4	50.3/45.3	50.4/45.8	46.4/42.0	45.3/41.3	44.8/39.4	48.8/35.0	4.73	.951	.356	.185
				50.4/34.2	52.2/47.8	56.8/53.3	53.3/50.0	51.4/48.4	48.6/44.3	60.8/52.0				
				60.7/52.4	55.8/52.8	64.4/62.3	61.8/59.8	59.7/58.0	55.0/52.4	74.1/69.4				
				69.5/65.6	60.8/59.1	69.9/68.9	67.8/66.9	66.0/65.1	61.6/60.3	76.8/74.4				
							37.6							
							4.83							
							1.94							
							.505							

TABLE II.15 A Posteriori Density Sigmas
21 Short Data Arcs (Data Noise = .05 cm/sec)
Adjusted parameters and a priori sigmas: 49 density blocks, σ = 100 mgal

Satellite States σ_{POS} = 10

σ_{VEL}[HCL] = (.01, .01, 2)

Unadjusted parameters and uncertainties: 176 density blocks, σ = 100 mgal

							-.0377							
							-.0987							
							-.3279							
							-1.628							
				2.393 2.193	4.027 3.937	3.872 3.779	4.185 4.101	4.477 4.401	4.321 4.239	2.795 2.633				
				5.156 5.097	3.299 3.240	3.248 3.190	3.198 3.139	3.223 3.164	3.480 3.425	6.712 6.675				
				4.364 4.304	2.692 2.627	2.380 2.310	2.394 2.325	2.436 2.369	2.710 2.648	5.778 5.744				
-.0059	-.0127	-.0312	-.0960	5.750 5.712	2.642 2.583	2.448 2.387	2.457 2.396	2.459 2.399	2.653 2.596	7.178 7.154	-.0214	-.0181	-.0096	-.0050
				4.125 4.060	2.667 2.603	2.291 2.220	2.251 2.179	2.248 2.175	2.640 2.577	5.955 5.922				
				5.021 4.959	3.683 3.630	3.597 3.545	3.573 3.522	3.588 3.537	3.820 3.770	6.804 6.769				
				2.221 2.001	4.162 4.076	4.332 4.251	4.058 3.971	3.811 3.716	4.441 4.362	3.249 3.115				
							-1.425							
							-.2748							
							-.0777							
							-.0281							

TABLE II.16 A Posteriori Density Sigmas
21 Short Data Arcs (Data Noise = .05 cm/sec)
Adjusted parameters and a priori sigmas: 49 density blocks, σ = 1 mgal

Satellite States, σ_{POS} = 10

σ_{VEL}[HCL] = (.01, .01, 2)

Unadjusted parameters and uncertainties: 176 density blocks, σ = 50 mgal

							.00068							
							.00111							
							.00824							
							.0650							
				15.917 .554	11.911 .419	10.787 .480	10.305 .493	9.889 .501	11.075 .454	14.302 .545				
				19.239 .403	14.376 .308	13.793 .336	13.253 .345	12.690 .356	13.978 .319	18.002 .413				
				21.796 .256	16.290 .243	15.965 .233	15.380 .232	14.700 .250	16.020 .227	20.595 .245				
.00111	.00203	.00110	.00770	22.186 .160	16.704 .241	16.359 .253	15.773 .246	15.076 .258	16.371 .221	20.926 .123	.0311	.00621	.00222	.00113
				20.952 .288	16.086 .281	15.374 .351	14.834 .347	14.213 .347	15.490 .287	19.543 .330				
				17.937 .448	14.075 .367	12.829 .479	12.384 .478	11.925 .471	13.140 .398	16.267 .507				
				15.226 .593	11.508 .474	9.673 .586	9.363 .582	9.097 .574	10.233 .514	12.492 .618				
							.2206							
							.0293							
							.0121							
							.0031							

TABLE II.17 A Posteriori Density Sigmas
21 Short Data Arcs (Data Noise - .05 cm/sec)
Adjusted parameters and a priori sigmas: 49 density blocks, σ = 50 mgal

Satellite States, σ_{POS} = 10

σ_{VEL}[HCL] = (.01, .01, 2)

Unadjusted parameters and uncertainties: 176 density blocks, σ = 1 mgal

							-.04							
							.04							
							.4							
			49.7 .8	43.5 4.1	29 7.2	27 7.3	27 7.2	27 7.4	28 7.5	40 6.3	49 1.6			
			47 2	25 3.7	17 1.7	17 1.9	17 1.8	17 1.8	17 1.7	21 2.4	43 4.0			
			44 3.0	23 3.1	17 1.5	17 1.6	16 1.4	16 1.5	17 1.5	20 1.7	35 6.0			
			44 2.2	23 2.2	18 1.4	17 1.5	17 1.2	17 1.3	18 1.4	21 .98	33 5.3			
.06	.1	.02	43 2.8	23 1.7	18 1.4	18 1.5	17 1.2	17 1.3	18 1.4	21 .9	32 5.6	.07	.07	.05
			45 2.1	23 2.7	18 1.5	17 1.7	17 1.3	17 1.6	17 1.5	21 2.0	32 5.5			
			45 2.7	23 3.6	17 1.6	17 2.0	17 1.5	16 1.8	17 1.7	20 2.5	35 6.2			
			48 1.9	25 3.9	17 1.8	17 2.1	16 1.7	17 2.0	17 1.9	21 2.7	43 4.1			
			49.6 .8	42 4.5	28 7.5	26 7.5	26 8.1	26 7.3	27 7.6	39 6.9	49 1.9			
							.06							
							.3							
							.02							

TABLE II.18 A Posteriori Density Sigmas
21 Short Data Arcs (Data Noise = .05 cm/sec)
Adjusted parameters and a priori sigmas: 81 density blocks, σ = 50 mgal

Satellite States σ_{POS} = 10

σ_{VEL} [HCL] = (.01, .01, 2)

Unadjusted parameters and uncertainties: 144 density blocks, σ = 50 mgal

							.007							
							.01							
							.03							
							.08							
				.79 / .29	.64 / .37	.61 / .37	.61 / .39	.61 / .39	.63 / .39	.71 / .31				
				.54 / .34	.52 / .35	.52 / .36	.52 / .37	.52 / .36	.53 / .36	.55 / .36				
				.53 / .26	.49 / .28	.49 / .29	.49 / .29	.49 / .28	.50 / .29	.53 / .30				
-.002	-.002	-.003	-.003	.52 / .20	.45 / .21	.44 / .21	.44 / .21	.44 / .21	.45 / .22	.50 / .25	.0004	-.002	-.002	-.001
				.48 / .18	.38 / .14	.36 / .13	.36 / .12	.36 / .12	.38 / .14	.45 / .22				
				.48 / .23	.34 / .15	.32 / .14	.32 / .14	.32 / .14	.33 / .15	.44 / .25				
				.79 / .25	.49 / .25	.45 / .25	.46 / .25	.46 / .24	.48 / .24	.65 / .29				
							-.13							
							-.02							
							-.004							
							-.001							

TABLE II.19 A Posteriori Density Sigmas

21 Short Data Arcs (Data Noise = .01 cm/sec)

Adjusted parameters and a priori sigmas: 49 density blocks, σ = 1 mgal

Satellite States, σ_{POS} = .001

σ_{VEL} = .001

Unadjusted parameters and uncertainties: 176 density blocks, σ = 1 mgal

							.004							
							.008							
							.016							
			.997 .013	.939 .064	.858 .112	.841 .100	.835 .098	.835 .101	.850 .113	.912 .080	.994 .020			
			.991 .015	.767 .046	.585 .061	.551 .056	.545 .058	.543 .059	.567 .061	.688 .053	.980 .019			
			.983 .027	.504 .072	.459 .057	.449 .058	.448 .058	.450 .058	.458 .058	.495 .072	.963 .035			
			.980 .027	.505 .057	.452 .051	.444 .051	.443 .049	.445 .050	.454 .053	.493 .060	.942 .046			
-.0013	-.0018	-.0026	.983 .021	.509 .046	.431 .046	.416 .041	.414 .038	.415 .040	.428 .047	.482 .055	.949 .035	-.0020	-.0016	-.0019
			.980 .019	.479 .049	.373 .045	.353 .035	.350 .032	.349 .034	.366 .045	.441 .055	.936 .041			
			.985 .018	.473 .059	.336 .054	.313 .042	.311 .041	.312 .042	.329 .052	.419 .063	.959 .031			
			.992 .014	.776 .040	.476 .070	.443 .058	.447 .058	.452 .058	.471 .067	.632 .057	.978 .021			
			.998 .006	.957 .040	.892 .072	.870 .062	.871 .061	.875 .060	.888 .069	.928 .059	.996 .013			
							-.0095							
							-.0014							
							-.0002							

TABLE II.20 A Posteriori Density Sigmas
21 Short Data Arcs (Data Noise - .01 cm/sec)
Adjusted parameters and a priori sigmas: 81 density blocks, σ = 1 mgal

Satellite States, σ_{POS} = .001

σ_{VEL} = .001

Unadjusted parameters and uncertainties: 144 density blocks, σ = 1 mgal

SET III.

Solution set III utilizes a 17 x 17 rectangular array of 5° x 5° density blocks with 31 independent data arcs giving data coverage over the center 49 blocks. The adjusted parameters in this set consist of the 372 satellite epoch state parameters plus various configurations of adjusted blocks over the data region. The principal design of this solution set is to display the effect of increasing the data region relative to that of Solution set II for both small (1 mgal) and large (50 mgal) a priori density block sigmas. All solutions have small a priori Cartesian error components on the arc states (.001 meters and .001 meters/sec for position and velocity, respectively).

Table III.1 displays the disastrous effect of estimating a subset of blocks within the data region, as most of the a posteriori sigmas of the recovered blocks are greater than their a priori values. It is clear that processing data which is over the unadjusted blocks and therefore strongly influenced by them should result in more significant aliasing errors on the adjusted set of blocks.

Tables III.2 through III.4 display estimation regions with no buffer layer, one buffer layer and two buffer layers, respectively, for the case of one mgal a priori error sigma on the density blocks. The recovered sigmas of the central adjusted region compare very closely with the same configurations of Solution Set II (Tables II.1 through II.3) with a smaller region of data coverage. Tables III.5 through III.7 repeat the same estimation region configurations, but with a large a priori uncertainty of 50 mgal on the density blocks. Comparing with the similar sets in Solution Set II (Tables II.9 through II.11) shows that increasing the data region with a poor estimation strategy (no buffer layer or only one buffer layer) and a large a priori uncertainty on the density blocks can result in considerably increased aliasing errors. The region covered by data in Solution Set III is nearly twice that of Set II, so that there are correspondingly more unadjusted blocks to contaminate the estimation accuracy when a poor strategy is used. It should be noted that Table III.7, with two buffer layers, again compares very closely with Table II.11, which has the same configuration but a smaller data region.

								÷0012								
								÷0036								
								÷0141								
								÷0863								
								÷2263								
								÷6928								
						1.449 1.436	1.055 1.026	.942 .910	1.054 1.026	1.419 1.405						
						1.905 1.896	1.414 1.392	1.171 1.143	1.394 1.372	1.846 1.838						
÷0016	÷0035	÷0093	÷0294	÷1006	÷1939	2.011 2.000	1.433 1.403	1.139 1.101	1.392 1.363	1.913 1.901	÷1880	÷0872	÷0241	÷0078	÷0030	÷0014
						1.847 1.839	1.379 1.358	1.133 1.106	1.335 1.314	1.773 1.764						
						1.487 1.477	1.036 1.012	.886 .855	1.003 .978	1.109 1.398						
								.6066								
								÷1771								
								÷0805								
								÷0144								
								÷0042								
								÷0016								

TABLE III.1 A Posteriori Density Sigmas
31 Short Data Arcs (Data Noise = .05 cm/sec)
Adjusted parameters and a priori sigmas: 25 density blocks, σ = 1 mgal

Satellite States, σ_{POS} = .001

σ_{VEL} = .001

Unadjusted parameters and uncertainties: 264 density blocks, σ = 1 mgal

								.0045								
								.0076								
								.0131								
								.0160								
								.0521								
					.936 .889	.755 .687	.679 .598	.659 .574	.666 .584	.722 .651	.892 .840					
					.993 .933	.750 .658	.668 .559	.650 .536	.657 .546	.733 .640	.945 .880					
					1.106 1.033	.712 .573	.618 .444	.614 .438	.614 .439	.688 .543	.943 .852					
-.0007	0	.0031	.0166	.0593	1.124 1.053	.679 .526	.566 .351	.557 .345	.553 .340	.618 .445	.884 .783	.0393	.0082	.0007	-.0008	-.0010
					1.010 .941	.661 .530	.530 .342	.504 .300	.506 .305	.565 .402	.784 .686					
					.844 .790	.664 .583	.522 .405	.472 .336	.488 .361	.561 .460	.703 .632					
					.794 .756	.617 .552	.504 .414	.472 .374	.484 .391	.548 .471	.708 .661					
								-.2102								
								-.0655								
								-.0124								
								-.0037								
								-.0051								

TABLE III.2 A Posteriori Density Sigmas
31 Short Data Arcs (Data Noise = .05 cm/sec)
Adjusted parameters and a priori sigmas: 49 density blocks, σ = 1 mgal

Satellite States, σ_{POS} = .001

σ_{VEL} = .001

Unadjusted parameters and uncertainties: 240 density blocks, σ = 1 mgal

								.0026								
								.004								
								.005								
								-.0069								
				.833 .188	.760 .118	.753 .075	.761 .076	.759 .078	.754 .078	.754 .075	.772 .096	.868 .153				
				.554 .292	.498 .164	.490 .172	.489 .159	.488 .163	.488 .168	.492 .170	.512 .153	.588 .230				
				.543 .282	.473 .106	.467 .107	.464 .105	.464 .107	.465 .106	.468 .104	.482 .092	.555 .227				
				.544 .255	.485 .105	.480 .101	.479 .101	.479 .105	.479 .101	.481 .098	.494 .092	.557 .204				
-.0011	-.0016	-.0025	-.0049	.533 .245	.477 .093	.472 .083	.472 .085	.471 .088	.471 .083	.473 .080	.484 .084	.548 .193	-.0032	-.0021	-.0015	-.0011
				.518 .269	.441 .076	.435 .055	.436 .056	.435 .056	.434 .053	.435 .052	.448 .066	.531 .210				
				.483 .285	.382 .074	.370 .042	.371 .041	.370 .039	.370 .039	.371 .040	.389 .065	.506 .225				
				.459 .263	.370 .113	.354 .104	.354 .101	.354 .107	.353 .105	.355 .104	.387 .117	.521 .222				
				.687 .240	.575 .168	.565 .156	.555 .139	.553 .136	.557 .146	.556 .155	.583 .164	.766 .185				
								-.0551								
								-.0122								
								-.0041								
								-.0018								

TABLE III.3 A Posteriori Density Sigmas
31 Short Data Arcs (Data Noise = .05 cm/sec)
Adjusted parameters and a priori sigmas: 81 density blocks, σ = 1 mgal

Satellite States, σ_{POS} = .001

σ_{VEL} = .001

[redacted]ju[redacted] pa[redacted]te[redacted]d [redacted]rta[redacted]es:[redacted]8 [redacted]ty[redacted]cks[redacted] = [redacted]l [redacted]

								.0018								
								.0025								
								.0020								
			.995 .019	.968 .045	.951 .060	.948 .060	.954 .055	.953 .056	.950 .059	.948 .060	.957 .053	.978 .035	.997 .013			
			.984 .019	.829 .047	.758 .035	.753 .015	.760 .011	.758 .012	.753 .013	.754 .017	.772 .029	.866 .044	.994 .009			
			.957 .036	.538 .076	.491 .041	.481 .042	.481 .040	.481 .041	.480 .041	.483 .041	.507 .042	.582 .067	.983 .022			
			.938 .054	.522 .065	.469 .029	.463 .031	.460 .031	.460 .032	.461 .031	.464 .030	.479 .028	.548 .063	.976 .030			
			.942 .045	.529 .055	.482 .029	.477 .029	.475 .029	.475 .029	.476 .029	.478 .029	.491 .027	.552 .052	.978 .026			
-.0009	-.0013	-.0019	.940 .043	.521 .053	.475 .027	.470 .023	.470 .022	.469 .023	.469 .022	.471 .023	.483 .026	.544 .048	.977 .023	-.0017	-.0012	-.0009
			.936 .051	.501 .063	.440 .027	.434 .018	.435 .016	.434 .016	.434 .016	.435 .018	.447 .027	.526 .057	.973 .028			
			.934 .053	.462 .072	.381 .032	.370 .021	.371 .019	.370 .018	.370 .019	.371 .020	.389 .033	.499 .065	.972 .030			
			.960 .031	.447 .072	.368 .042	.352 .035	.352 .033	.351 .034	.351 .034	.354 .035	.385 .045	.515 .064	.981 .021			
			.984 .020	.679 .075	.570 .056	.561 .045	.552 .041	.550 .041	.554 .042	.562 .046	.579 .059	.763 .059	.994 .097			
			.995 .018	.964 .048	.948 .056	.950 .050	.948 .050	.942 .053	.946 .051	.950 .050	.951 .053	.972 .039	.997 .012			
								-.0092								
								-.0029								
								-.0012								

TABLE III.4 A Posteriori Density Sigmas
31 Short Data Arcs (Data Noise = .05 cm/sec)
Adjusted parameters and a priori sigmas: 121 density blocks, σ = 1 mgal

Satellite States, σ_{POS} = .001

σ_{VEL} = .001

Unadjusted parameters and uncertainties: 168 density blocks, σ = 1 mgal

								.533								
								.810								
								1.163								
								-1.38								
								33.11								
					130.1 130.1	192.9 192.9	141.5 141.5	95.9 95.9	116.5 116.5	155.8 155.8	117.5 117.5					
					200.6 200.6	306.0 306.0	228.9 228.9	150.3 150.3	184.2 184.2	244.4 244.4	178.4 178.4					
					267.8 267.8	390.9 390.9	289.7 289.7	187.9 187.9	229.6 229.6	304.9 304.9	224.8 224.8					
.239	.984	3.678	14.72	47.89	285.0 285.0	410.3 410.3	303.6 303.6	195.9 195.9	237.0 237.0	312.2 312.2	227.5 227.5	34.70	8.786	1.816	.276	-.072
					250.3 250.3	366.2 366.2	271.5 271.5	174.8 174.8	208.7 208.6	271.8 271.8	189.8 189.8					
					173.5 173.5	266.5 266.5	198.2 198.2	127.9 127.9	151.1 151.1	193.0 193.0	122.5 122.4					
					96.2 96.2	149.0 149.0	110.3 110.3	72.7 72.7	84.9 84.9	108.1 108.1	69.5 69.5					
								-14.9								
								-15.4								
								-2.26								
								-.561								
								-.234								

TABLE III.5 A Posteriori Density Sigmas
31 Short Data Arcs (Data Noise = .05 cm/sec)
Adjusted parameters and a priori sigmas: 49 density blocks, σ = 50 mgal

Satellite States, σ_{POS} = .001

σ_{VEL} = .001

Unadjusted parameters and uncertainties: 240 density blocks, σ = 50 mgal

								.530								
								1.217								
								3.808								
								17.10								
				54.95 54.71	39.42 39.11	37.69 37.42	40.17 39.89	38.54 38.25	39.31 39.01	37.28 37.89	32.21 31.40	52.15 51.50				
				63.68 63.48	46.78 46.48	43.64 43.37	45.73 45.47	44.99 44.71	45.47 45.17	41.97 41.54	33.32 32.31	63.73 63.21				
				66.90 66.66	51.72 51.38	46.55 46.22	48.41 48.09	47.92 47.58	48.27 47.90	43.34 42.78	32.76 31.39	69.65 69.04				
				68.96 68.72	54.30 53.95	47.11 46.76	48.06 47.72	47.80 47.44	47.90 47.50	42.15 41.54	30.98 29.43	69.09 68.46				
-.179	-.414	-1.31	-4.92	68.72 68.51	53.08 52.76	44.11 43.78	44.13 43.80	43.92 43.57	43.81 43.42	37.92 37.32	27.56 26.00	63.32 62.73	-.147	-.008	-.001	-.010
				63.02 62.85	46.73 46.46	36.97 36.67	36.41 36.11	36.23 35.91	35.98 35.64	30.69 30.14	22.57 21.19	53.64 53.13				
				49.58 49.46	35.44 35.24	26.90 26.67	26.25 26.02	26.09 25.84	25.83 25.54	21.78 21.35	16.54 15.45	40.38 40.00				
				26.83 26.75	20.40 20.26	14.39 14.22	13.79 13.61	13.56 13.37	13.64 13.43	11.60 11.28	10.42 9.71	21.97 21.68				
				16.33 16.26	12.08 11.97	11.72 11.62	10.93 10.81	11.31 11.20	11.34 11.21	11.30 11.13	11.10 10.78	15.11 14.87				
								-29.0								
								-5.04								
								-1.25								
								-.424								

TABLE III.6 A Posteriori Density Sigmas
31 Short Data Arcs (Data Noise = .05 cm/sec)
Adjusted parameters and a priori sigmas: 81 density blocks, σ = 50 mgal

Satellite States, σ_{POS} = .001

σ_{VEL} = .001

Unadjusted parameters and uncertainties: 168 density blocks, σ = 50 mgal

								.153								
								.238								
								.445								
			43.77 7.02	32.45 8.24	21.92 7.51	20.94 7.64	20.95 7.66	21.11 7.52	20.81 7.44	21.09 7.67	22.80 7.84	36.34 8.04	47.64 3.86			
			32.21 8.92	15.38 2.40	11.65 1.80	11.14 1.93	11.13 1.81	11.16 1.83	11.32 1.84	11.86 1.90	12.91 1.99	19.92 2.84	41.53 4.96			
			23.16 10.29	13.96 2.28	10.64 1.82	10.05 1.93	10.22 1.72	10.27 1.75	10.49 1.75	11.24 1.90	12.45 1.99	17.72 2.28	30.55 90.2			
			23.27 9.78	13.10 2.28	9.89 1.70	9.21 1.81	9.50 1.53	9.56 1.55	9.84 1.54	10.73 1.78	12.17 1.94	17.56 2.09	29.13 9.07			
			22.84 9.62	12.57 2.34	9.32 1.60	8.57 1.64	8.88 1.33	8.94 1.34	9.20 1.34	10.11 1.62	11.72 1.88	16.16 2.27	29.42 8.22			
-.039	-.034	-.088	21.60 10.16	11.77 2.49	8.55 1.56	7.79 1.50	8.04 1.19	8.07 1.20	8.29 1.20	9.12 1.47	10.79 1.85	15.06 2.57	27.55 8.57	-.064	-.490	-.030
			20.29 10.75	10.53 2.65	7.34 1.58	6.61 1.40	6.80 1.15	6.78 1.17	6.95 1.17	7.65 1.39	9.30 1.86	13.72 2.87	27.13 9.05			
			18.37 10.79	8.88 2.81	5.76 1.67	5.14 1.41	5.24 1.24	5.20 1.25	5.32 1.25	5.89 1.42	7.43 1.92	11.61 3.08	26.17 9.39			
			17.38 9.19	7.47 2.93	4.44 1.79	3.96 1.50	3.89 1.40	3.90 1.39	4.01 1.39	4.48 1.53	5.76 2.02	9.34 3.26	28.50 8.29			
			28.21 6.33	8.14 3.05	5.00 1.90	4.61 1.61	4.33 1.54	4.46 1.53	4.58 1.54	4.92 1.65	5.76 2.11	9.58 3.42	41.13 5.61			
			43.26 7.94	27.40 11.63	17.05 9.52	16.24 9.50	15.21 9.25	15.73 9.55	16.01 9.64	16.19 9.32	17.17 8.97	29.61 10.80	47.10 4.46			
								.062								
								.092								
								.053								

TABLE III.7 A Posteriori Density Sigmas
31 Short Data Arcs (Data Noise - .05 cm/sec)
Adjusted parameters and a priori sigmas: 121 density blocks, σ = 50 mgal

Satellite States σ_{POS} = .001

σ_{VEL} = .001

Unadjusted parameters and uncertainties: 168 density blocks, σ = 50 mgal

SET IV.

Solution Set IV displays the error analysis for an estimator which ignores aliasing effects and assumes the satellite states to be perfectly known. This in some measure serves as a bridge between the results of Schwarz, Hajela and Solution Sets I and II, showing clearly how misleadingly optimistic the results of error analysis studies can be when important aliasing errors are neglected.

Table IV.1 examines the long data arc of Solution Set I with data over the center 25 block region. The twelve satellite state parameters are put into the unadjust category along with all density blocks outside of the data region with a zero a priori sigma. The total error is then the "noise only" contribution; the aliasing error is zero. The two numbers inside the twenty-five adjusted density blocks represent the recovered sigmas for the two cases of 1 mgal and 50 mgal a priori sigma for the adjusted blocks, respectively, i.e.

$$\sigma_{1\ \mathrm{mgal}} / \sigma_{50\ \mathrm{mgal}}$$

Unlike the cases of Sets I, II and III, the lack of a priori knowledge of the adjusted blocks has little impact on the estimation accuracy. Table IV.2 displays the correlation coefficients of the adjusted blocks with the center block for the case depicted in Table IV.1. The N-S and E-W patterns closely resemble the results of Schwarz.

Tables IV.3 and IV.4 correspond to the error analysis of Tables IV.1 and IV.2 with the exception that 21 independent data arcs are used in place of one long arc. Generally the same patterns result with the exception of the asymmetry introduced in the southern-most row due, as previously discusssed, to the variational equations for the density block parameters all starting from zero initial conditions at epoch. It should be noted that the long arc solution of Table IV.1 displays a superior estimation accuracy to the short arc solution of Table IV.2, even though the data coverage is the same. The reason for this, of course, is that the short arcs are assumed independent, while the consecutive passes of the long arc are correlated through the orbital dynamics.

The solution displayed in Table IV.3 corresponds quite closely with the solution 3.1 of Schwarz for 5° x 5° blocks with the low-low configuration at 300 km altitude when proper corrections are made for the different values used for the data noise and for the differences in data rates and data spacing. Noting that Schwarz used approximately one data arc per 5° x 5° block, an observation approximately every 30 seconds and a data noise of .005 cm/sec, a factor to relate his estimated density parameters to those of Table IV.3 would be

$$\left(\frac{.05}{.005}\right)\left(\frac{1}{\sqrt{4}}\right)\left(\frac{1}{\sqrt{6}}\right) \simeq 2 \quad .$$

Thus his estimated uncertainty of approximately .2 mgal should correspond to approximately .4 mgal for our results of IV.3. As the satellite altitude used in Table IV.3 was 250 km compared to 300 km used to Schwarz in solution 3.1, we would expect his values to be slightly larger than ours.

					.13 .13	.17 .18	.18 .19	.17 .18	.11 .12					
					.10 .10	.13 .13	.13 .13	.13 .13	.10 .10					
					.09 .10	.11 .12	.12 .12	.11 .12	.09 .09					
					.10 .10	.13 .13	.13 .13	.13 .13	.10 .10					
					.13 .14	.17 .18	.18 .19	.17 .18	.12 .12					

TABLE IV.1 A Posteriori Density Sigmas
One Long Data Arc (Data Noise = .05 cm/sec)
Adjusted parameters and a priori sigmas: 25 density blocks, $\sigma = \frac{1\ \text{mgal}}{50\ \text{mgal}}$

Unadjusted parameters: None

					-.01 -.01	.03 .03	-.04 -.04	.09 .09	-.08 -.07					
					-.05 -.05	.13 .13	-.31 -.31	.13 .14	-.05 -.05					
					.26 .27	-.60 -.61	1 1	-.60 -.61	.26 .27					
					-.05 -.05	.13 .13	-.31 -.31	.13 .13	-.05 -.05					
					-.04 -.04	.08 .08	-.04 -.03	.03 .02	-.001 .001					

TABLE IV.2 Correlations of Adjusted Blocks with Center Block
One Long Data Arc (Data Noise = .05 cm/sec)
Adjusted parameters and a priori sigmas: 25 density blocks, $\sigma = \frac{1 \text{ mgal}}{50 \text{ mgal}}$

Unadjusted parameters: None

.21 / .23	.27 / .31	.27 / .32	.26 / .30	.21 / .22
.16 / .18	.22 / .21	.23 / .28	.22 / .25	.15 / .16
.17 / .19	.24 / .28	.24 / .30	.23 / .27	.16 / .18
.16 / .17	.21 / .24	.21 / .25	.20 / .23	.14 / .15
.06 / .06	.08 / .09	.08 / .10	.07 / .09	.06 / .06

TABLE IV.3 A Posteriori Density Sigmas
21 Short Data Arcs (Data Noise = .05 cm/sec)
Adjusted parameters and a priori sigmas: 25 density blocks, $\sigma = \frac{1 \text{ mgal}}{50 \text{ mgal}}$

Unadjusted parameters: None

					.20 / .32	-.48 / -.60	.70 / .78	-.47 / -.58	.19 / .36					
					.30 / .42	-.54 / -.65	.64 / .78	-.54 / -.68	.29 / .41					
					.28 / .49	-.73 / -.79	1 / 1	-.73 / -.79	.37 / .47					
					.25 / .37	-.49 / -.61	.59 / .70	-.48 / -.59	.24 / .34					
					.30 / .41	-.57 / -.68	.75 / .82	-.58 / -.68	.31 / .42					

TABLE IV.4 Correlations of Adjusted blocks with Center Block
21 Short Data Arcs (Data Noise = .05 cm/sec)
Adjusted parameters and a priori sigmas: 25 density blocks, $\sigma = \frac{1 \text{ mgal}}{50 \text{ mgal}}$

Unadjusted parameters: None

7.0 SUMMARY

This study applied covariance error analysis techniques to investigate estimation strategies for the low-low-SST mission for accurate local recovery of gravitational fine structure, considering the effects of aliasing. A 5° x 5° surface density block representation of the high order geopotential was utilized with the drag-free "low-low" GRAVSAT configuration in a circular polar orbit at 250 km altitude.

Satellite-to-satellite relative range-rate data was used in the error analysis investigation, as the range data was found to be much less sensitive to fine structure recovery. A data noise of .05 cm/sec was assumed for most of the error analysis studies. No ground tracking data was included and satellite state accuracy requirements for the estimation of the density blocks were investigated in the error analysis by a priori error sigmas for the epoch states, both in Cartesian and HCL coordinates. The sensitivity of the data type to even very small a priori errors in the satellite epoch state velocities (.001 meters/sec) led to severe aliasing errors in the estimation of local sets of density blocks, forcing the satellite epoch state parameters to be included with the surface density parameters in the estimation process.

The SST relative range-rate data type exhibits strong recovery ability only for the along track components of velocity, the normal matrix being poorly conditioned for the recovery of radial and cross track components. This requires satellite orbital accuracies from other tracking means to a minimum of 10 meters in position and .01 meters/sec in radial and cross track velocity components.

The recovery of local sets of density blocks from long data arcs proved not to be feasible due to strong aliasing effects from non-estimated density blocks all along the ground track - even those very far removed from the set of estimated blocks. The error analysis for the recovery of local sets of density blocks using independent short data arcs demonstrated that the estimation strategy of simultaneously estimating a local set of density blocks covered by data and two "buffer layers" of density blocks not covered by data resulted in almost negligible aliasing errors on the estimation accuracy for blocks near the center of the recovered set due to unadjusted surface density blocks.

With an orbital accuracy of 10 meters in position, .01 meters/sec in radial and cross track velocity and 2 meters/sec in along track velocity obtained by other means of tracking, the low-low SST range-rate data, with a noise of .05 cm/sec, will recover $5° \times 5°$ surface density blocks to approximately 5 mgal and 17 mgal, respectively, when an a priori knowledge of the blocks to 15 mgal and 50 mgal is assumed. [Note: These values when multiplied by 2π give the approximation to the corresponding values of gravity anomaly blocks.] This is to be contrasted to results (Solution Set IV) predicting recovery to approximately .2 mgal (40 cm geoid) when the error analysis does not consider aliasing errors from unadjusted density blocks and assumes the satellite states to be perfectly known.

We would conclude that the estimation of gravitational fine structure by recovery of local sets of density blocks utilizing SST relative range rate data with the "low-low" drag-free satellite configuration is not a feasible approach, principally due to the very stringent orbital accuracies required with many short data arcs. The low altitude satellite orbits would make the attainment of such accuracy from ground tracking extremely difficult.

The possibility of supplying such tracking from a third high altitude satellite is a concept (the "high-low-low" configuration) which deserves investigation.

An investigation of the feasibility of a global recovery for the gravitational fine structure parameters, a concept summarily ruled out of hand by many authors due to the magnitude of the problem, also deserves attention. Such a procedure would eliminate the aliasing problem inherent with the estimation of local sets of parameters and relax the difficulty of obtaining dense coverage of very accurate ground tracking.

8.0 ACKNOWLEDGEMENT

It is with pleasure that the authors acknowledge the support of Dr. P. Argentiero of GSFC, whose error analysis techniques developed in his study of the recovery of local sets of gravity anomalies were used in this investigation. The assistance provided by Mr. Daniel Chin of BTS in modifying the ERODYN and GEODYN programs and by Mr. Tom Englar and Mr. Andy Jazwinski of BTS for interesting discussions is also acknowledged.

9.0 NEW TECHNOLOGY

The effort under this contract consisted of the application of covariance error analysis techniques for investigation of estimation strategies for the "low-low" SST mission for accurate local recovery of gravitational fine structure, considering the effects of aliasing errors. Frequent reviews and a final survey for new technology were performed. It is believed that the mathematical and programming techniques and algorithms developed do not represent "reportable items", or patentable items, within the meaning of the New Technology Clause. Our reviews and final survey found no other items which could be considered reportable items under the New Technology Clause.

10.0 REFERENCES

1. Argentiero, P., W. D. Kahn and R. Garza-Robles, "Strategies for Estimating the Marine GEOID from Altimeter Data," GSFC X-932-74-90, April 1974.

2. Chin, M. M., C. C. Goad and T. V. Martin, "GEODYN System Description", Volume I, Wolf Research and Development Corporation, Riverdale, Maryland. September 1972.

3. Eades, J.B., "Relative Motion of Orbiting Satellites," NASA CR-112113, July 1972.

4. Hajela, D. P., "Direct Recovery of Mean Gravity Anomalies from Satellite-to-Satellite Tracking," Department of Geodetic Science, Report No. 218, Ohio State University, December 1974.

5. Hatch, W.E. and Daniel Chin, "ERODYN Program Mathematical Description, Version 7507," ASGI-TR-75-07, NASA Contract NAS 5-20774, August 1975.

6. Heiskanen, W. A. and H. Moritz, Physical Geodesy, W. H. Freeman and Company, San Francisco, 1967.

7. Lancaster, E. R., "Relative Motion of Two Particles in Elliptic Motion," AIAA Journal, Vol. 8, No. 10, October 1970.

8. Lowrey, B. E., "Twinsat Earth Gravity Field Mapping," GSFC X-932-75-279, October 1975.

9. Schwarz, C.R., "Gravity Field Refinement by Satellite-to-Satellite Doppler Tracking," Department of Geodetic Science, Report No. 147, Ohio State University, Columbus, December 1970.

PRECEDING PAGE BLANK NOT FILMED

BUSINESS AND TECHNOLOGICAL SYSTEMS, INC.
10210 GREENBELT ROAD • SEABROOK • MARYLAND 20801
301/794-8800